Thermodynamic assessment of the Mo-S system and its application in thermal decomposition of MoS_2

Senlin Cui [1], Biao Hu [2], Bin Ouyang [3], and Dongdong Zhao [4]

1 Department of Aerospace Engineering, Iowa State University, 537 Bissell Road, Ames, Iowa 50011, USA

2 School of Materials Science and Engineering, Anhui University of Science and Technology, Huainan, Anhui, 232001, China

3 National Center for Supercomputing Applications, University of Illinois at Urbana–Champaign, 1205 W Clark St, Urbana, Illinois 61801, USA

4 Department of Materials Science and Engineering, Norwegian University of Science and Technology (NTNU), 7491 Trondheim, Norway

Corresponding author: Senlin Cui, slcui@iastate.edu (S. Cui)

Abstract

The Mo-S system is crucial to extractive metallurgy, tribology, and various possible applications in design and fabrication of novel two-dimensional (2D) materials. First-principles calculations were utilized to compute the enthalpies of formation of molybdenum sulfides at 0 K and the heat capacity of Mo_2S_3 up to 960 K. A critical evaluation of the thermodynamic properties, phase equilibria, and phase diagram information in the literature was carried out to facilitate the thermodynamic optimization of the Mo-S system. The obtained thermodynamic description of the Mo-S system can satisfactorily represent most of the reliable thermodynamic and phase diagram information. Pressure-temperature (*P*-*T*), pressure-composition (*P*-*x*), and temperature-composition (*T*-*x*) diagrams of the Mo-S system were utilized to study the thermal decomposition of MoS_2 for raw Mo production. Reduced pressure and high temperature are thermodynamically favorable conditions for the MoS_2 reduction process.

Key words:

The Mo-S system; First-principles calculations; Phase diagram; Thermodynamic assessment, Thermal decomposition of MoS_2.

1 Introduction

The Mo-S system is very attractive due to its importance in extractive metallurgy, tribology, and various possible applications in design and fabrication of novel two-dimensional (2D) materials. MoS_2 (molybdenum disulfide) mineral is the major resource for the extraction of Mo and rare metal Re [1-4] which have important applications in aerospace industry [2, 4]. MoS_2 has a lamellar structure which is formed by van der Waals force bonding of many stacked layers [5]. The high strength covalent bonds within the layer make it easy to slide rather than be destroyed. MoS_2 is therefore well-known as solid lubricant with a lubricity comparable to graphite [5-8] and as nanoscale additive of lubricating oil [9]. Besides, MoS_2 as a 2D material exhibits excellent optoelectronic [8, 10-14], piezoelectronic [15], and valleytronic [10] properties. In addition, the possibility of tuning structural phase within MoS_2 lattice offers wider space and more flexibility for manipulating properties [16-19]. Thus, there are great potential applications of MoS_2 in solar energy harvesting and conversion [8, 10, 13], photon detectors [10, 13], photon catalysis [13], transistor [8, 11, 20, 21], light emitter [14, 20], modular [20], etc.

Another layer crystal structured [22] molybdenum sulfide phase Mo_2S_3 (molybdenum sesquisulfide) was utilized to synthesis nanorods [23]. The nanostructured Mo_2S_3 is of interest in the applications as catalysis, electrodes, and intercalation hosts. In addition, the metastable Mo_3S_4 (molybdenum tetrasulfide) phase has potential applications as superconductor [24].

During the synthesis or fabrication of nanostructured molybdenum sulfide material or 2-D layered device, the methods like solid/gas reaction [23], chemical vapor deposition (CVD) [12, 20], low pressure CVD [20], plasma enhanced CVD [20], etc., may be utilized. Thermodynamic and kinetic information of the Mo-S system is of fundamental importance in controlling the rate of chemical reactions involved, and the thickness and homogeneity of the layer of 2D material [25] as well as in understanding the gas/solid interaction during the fabrication process. Furthermore, the traditional Mo production process has unsolved problems such as long production cycle, complex purification procedure, low yield, and pollution due to H_2S and SO_2 [26]. The eco-friendly, low energy consumption, and high resource utilization Mo extraction process such as vacuum thermal decomposition of MoS_2 is under further development [26, 27]. Pressure and

temperature are among the determinant factors of the thermal decomposition process [26-29]. Thus, knowledge of phase equilibria in the Mo-S system under varying temperature, composition, and pressure is the prerequisite for the design and control of various related material fabrication and metallurgical processes.

The present study attempts to build the Mo-S phase diagram with the aid of CALPHAD (CALculation of PHase Diagram) [30-35] approach, get a set of Gibbs energy functions that can represent the equilibrium state of the Mo-S system, and study the thermal decomposition process of MoS_2. A comprehensive literature review and critical evaluation is carried out for the thermodynamic, phase equilibria, and phase diagram measurements related to the Mo-S system. First-principles calculations are utilized to solve the controversial issues related to the phase stability and supplement the evaluation and optimization work. A set of thermodynamic parameters for the Mo-S system is obtained to describe the thermodynamic properties and phase diagram information. The thermal decomposition process of MoS_2 is studied based on the calculated pressure-temperature (*P*-*T*), pressure-composition (*P*-*x*), and temperature-composition (*T*-*x*) diagrams.

2 First-principles calculations

The highly efficient first-principles calculations method as implemented in the Vienna Ab initio Simulation Package (VASP) [36, 37] was utilized to determine the ground-state enthalpies of formation and the heat capacity of the Mo-S intermetallics. The frozen-core Projector Augmented Wave method (PAW) [38, 39] was adopted to depict the electron-ion interactions, and the exchange-correlation was described by the Generalized Gradient Approximation (GGA) of Perdew-Burke-Ernzerhof (PBE) [40]. Plane wave cut-off energy was set to be 400 eV to make sure the total energy differences were less than 1 meV/atom for all the compounds. The integration of the Brillouin zone (BZ) was conducted on the basis of the Monkhorst-Pack scheme [41] *k*-points sampling in combination with the linear tetrahedron method including Blöchl corrections [42].

For enthalpies of formation calculations at 0 K, full relaxations with respect to volume, the shape of unit cell, and the atomic positions were carried out on the unit cells of the Mo-S

compounds till the Hellmann-Feynman force on all atoms was $<10^{-2}$ eV/Å. The enthalpies of formation for the Mo-S compounds were calculated using the following equation:

$$\Delta H_f(Mo_mS_n) = E(Mo_mS_n) - \left[\frac{m}{m+n}E(Mo) + \frac{n}{m+n}E(S)\right] \quad (1)$$

where $E(Mo_mS_n)$, $E(Mo)$, and $E(S)$ represent the total energies of Mo_mS_n, Mo, and S, respectively, in their equilibrium state. It should be noted that the reference states are bcc_A2 Mo and orthorhombic S. The calculated enthalpies of formation of the Mo-S compounds at 0 K are listed in Table 1.

After structural optimization, phonon calculations of α_Mo_2S_3 (*Monoclinic*) have been performed to evaluate the vibrational frequencies [43, 44]. A 2×2×2 supercell was constructed to obtain force constants with the criteria of convergence set as 10^{-8} eV. With the obtained force constant matrix, the vibrational frequency $\omega(q)$, can be calcualted by solving the secular equation:

$$\left|\frac{1}{\sqrt{m_1 m_2}}\tilde{C}_{IA,IB}(q) - \omega^2(q)\right| = 0 \quad (2)$$

where m_1 and m_2 are the atomic masses of atoms *1* and *2*, respectively.

With the vibrational frequencies, the Helmholtz free energy F_{phonon} is given as:

$$F_{phonon} = \frac{1}{2}\sum_{q,v}\hbar\omega_{q,v} + k_B T\sum_{q,v}\ln\left[1 - \exp(-\hbar\omega_{q,v}/k_B T)\right] \quad (3)$$

where q and v are the wave vector and band index, respectively, $\omega_{q,v}$ is the phonon frequency at q and v, and T is the temperature in Kelvin. k_B and $\hbar$ are the Boltzmann constant and the reduced Planck constant, respectively. Under quasi-harmonic approximation (QHA), the Gibbs energy at constant pressure can then be formulated as:

$$G(T,P) = \min_V \left[U(V) + F_{phonon}(T;V) + PV \right] \quad (4)$$

The heat capacity under constant pressure can then be calculated as:

$$C_P(T,P) = -T \frac{\partial^2 G(T,P)}{\partial T^2} \quad (5)$$

The calculated heat capacity of α_Mo_2S_3 under 1 bar from 0 to 960 K in the present work is listed in Table 1 in the supplementary data, and shown in Fig. 1. The derived entropy of α_Mo_2S_3 at 298.15 K is shown in Table 1.

3 Critical evaluation of literature information

3.1 Thermodynamic information

3.1.1 Thermodynamic properties of MoS_2

Thermodynamic data of MoS_2 (*Hexagonal*) available in the literature include heat capacity, heat content, entropy of formation, enthalpy of formation, and Gibbs energy of formation. These experimental data are summarized in Table 1 and Figs. 1 to 4, and are briefly discussed as follows.

The measured low temperature heat capacity data of MoS_2 at 5-350 K from different groups [45-48] via adiabatic calorimetry are in good agreement. The experimental heat content data of MoS_2 are available in the temperature range of 525-1973 K [49-51]. The derived heat capacity of

MoS_2 from these heat content data [49-51] are also consistent with the low temperature heat capacity data [45-48]. The first-principles calculations data from Yuan et al. [52] and Ali et al. [53] show deviation from the experimental data at high temperature, see Fig. 1(a). (It should be noted that the data from Yuan et al. [52] is under constant volume.)

Entropies of MoS_2 at 298.15 K derived from low temperature adiabatic calorimetry data [45, 48-50, 54] are generally in good agreement. The value derived from electron motive force (emf) data by Makolkin [55] for MoS_2 is slightly higher, while the indirect data from Hager and Elliott [56] systematically show positive deviation from other data.

The enthalpy of formation of MoS_2 at 298.15 K was measured by O'hare et al. [57, 58] using a fluorine bomb calorimeter and Makolkin [55] using electron motive force (emf) measurements. Sukhushina and Vasil'eva [59], Bartovská and Černý [60], Schaefer and Gokcen [61, 62], and Stubbles and Richardson [63] also reported the derived enthalpy of formation from their Gibbs energy of formation data. However, most of the reported enthalpy of formation data show deviation from the calorimetry ones [57, 58]. The first-principles calculations data from Pan and Guan [64] also show certain acceptable difference with the experimental data. The data reported by Bartovská and Černý [60] and Schaefer and Gokcen [61, 62] are consistent with the calorimetry data. The first-principles calculations data from Shang et al. [25] and the present work are in good agreement with the calorimetry data. The data reported by Stubbles and Richardson [63] is quite negative which may be due to S_2 gas was used as the reference state for S.

The Gibbs energy of formation of MoS_2 in the heterogeneous equilibrium of Mo/S_2 (gas)/MoS_2 was investigated by Pouillard and Perrot [65], Larson and Elliott [66], Schaefer and Gokcen [61, 62], Sukhushina and Vasil'eva [59], Bartovská and Černý [60], Suzuki et al. [67], Zelikman and Krein [68], Parravano and Malquori [69, 70], and Isakova [71]. Most of these experimental data are in good agreement. However, certain scatter is shown. The earlier data from Zelikman and Krein [68], Parravano and Malquori [69, 70], and Isakova [71] are inconsistent with the later data. In the early investigation by Parravano and Malquori [69, 70], a wrong reaction constant for $2H_2S = 2H_2 + S_2$ was used during the thermodynamic calculations [68] and the measurements may be not related to MoS_2 but Mo_2S_3 [60, 63] since MoS_2 was considered as the

lowest compound in their work. Besides, these deviations may be also due to the large experimental errors during the measurements.

3.1.2 Thermodynamic properties of Mo_2S_3

The reported thermodynamic properties of Mo_2S_3 are limited to enthalpy of formation and Gibbs energy of formation. The enthalpy of formation of Mo_2S_3 at 298.15 K was deduced by O'hare et al. [57] from the literature data. This value is quite close to the prediction using those of MoS_2 and Mo. The presently calculated value from first-principles calculations is quite close to the suggested value by O'hare et al. [57].

The Gibbs energy of formation of Mo_2S_3 was measured by McCabe [72], Stubbles and Richardson [63], Hager and Elliott [56], Pouillard and Perrot [65], Suzuki et al. [67], and refined by Sukhushina and Vasil'eva [59]. These data are in excellent agreement except for the data from McCabe [72] show certain discrepancy. There is no report of Mo_2S_3 heat capacity measurements till now. The present first-principles data are the only available information.

3.2 Phase diagram data

The Mo-S phase diagram was evaluated by Moh and Takeno [73, 74], Brewer and Lamoreaux [75], Johnson et al. [76], and Starkov et al. [77]. It can be seen from the literature that the Mo-S phase diagram is still largely undetermined in the high temperature region. It could mainly due to the extremely high melting point of Mo, and the high vapor pressure of S and the difficulty in controlling it. Moh and Takeno [73, 74] proposed a first version of Mo-S phase diagram in the range of Mo-MoS_2 based on their own experimental data and literature information. According to Moh and Takeno [73, 74], there is a stable liquid miscibility gap in the Mo rich side, and an eutectic reaction between liquid, Mo, and Mo_2S_3. Mo_2S_3 forms incongruently and has a polymorphic transition. MoS_2 melts congruently at a very high temperature. Later, Brewer and Lamoreaux [75] optimized the Mo-S system and presented the Mo-S phase diagram under 1 bar. The Mo_2S_3 phase forms congruently and MoS_2 incongruently from liquid and gas. There is no liquid miscibility gap in the Mo rich liquid. Johnson et al. [76] also reviewed the Mo-S phase

diagram but with a polymorphic transition of the MoS_2 phase. In the evaluation of Starkov et al. [77], Mo_2S_3 forms incongruently and MoS_2 via a peritectoid reaction at 1300 °C. The phase diagram studies in the Mo-S system are summarized in Table 2. And the measured invariant temperatures are listed in Table 3.

3.2.1 The compound phases

Mo_2S_3 is the lowest compound in the Mo-S binary system [78]. And this phase is hard to fabricate using Mo and MoS_2 below 900 °C [79]. The Mo_2S_3 phase did not decompose after annealed at 600 °C for 21 days [80]. The composition of Mo_2S_3 was reported to be $Mo_{2.06}S_3$ by Morimoto and Kullerud [79] at 935 °C, $MoS_{1.457}$ by Suzuki et al. [67], and $Mo_2S_{3-\delta}$ ($0.008 \leq \delta \leq 0.036$) by Krabbes et al. [81]. Mo_2S_3 has the exact stoichiometry when the possible experimental error is considered. There is no consensus about the melting temperature of Mo_2S_3. It can be seen from Table 3 that the reported melting temperatures vary from 1600 to 1780 ºC. Congruent melting [82, 83], incongruent melting [73, 84, 85], and dissociation to Mo and gas [78] were reported. The phase diagram evaluations carried out by Johnson et al. [76] and Starkov et al. [77] also showed more than hundred degree's difference. It seems very hard to justify the melting behavior and temperature of the Mo_2S_3 phase based on the literature information. And the Mo_2S_3 phase is unstable at low temperature and dissociates via an eutectoid reaction to Mo and MoS_2 at 610±5 °C [79, 84] by phase diagram measurements or 664 °C [65] by thermodynamic calculations using high temperature thermodynamic data. The present work prefers the phase diagram measurements [79, 84].

Two polymorphous namely rhombohedral 3R_MoS_2 and hexagonal 2H_MoS_2 were found in natural minerals [86] and synthesized in experiments [87-89]. And the 3R_MoS_2 was reported to be richer in Mo than 2H_MoS_2 [90, 91]. The 3R_MoS_2 when heating up will undergo polymorphic transition to 2H_MoS_2 [89, 91]. This rises the controversy about the stability of 3R_MoS_2 compared to 2H_MoS_2 at low temperature. For instance, a transition temperature of about 500 ºC [91] or about 1000 °C [76] was reported. In addition, 2H_MoS_2 was reported to be stable down to room temperature [79]. In fact, 3R_MoS_2 is very rare in natural molybdenite and always contains high percentage of Re [86, 92, 93]. 3R_MoS_2 could be stabilized due to the

presence of Re [88]. Besides, the crystal growth experiments [76] may also produce metastable crystals. The present first-principles calculations indicate that 2H_MoS_2 is stable than 3R_MoS_2 at 0 K (see Table 1). Consequently, the present work considers that the 2H_MoS_2 is stable down to room temperature.

Morimoto and Kullerud [79], Rau [94], and Yamamoto et al. [95] reported that MoS_2 is a stoichiometric compound. Ugryumova et al. [96], Red'ko et al. [97], Suzuki et al. [67], and Schaefer et al. [80] indicated that MoS_2 has a narrow homogeneity range of 64.91-69.09 at% S at high temperature (900-1284 ºC). Mering and Levialdi [98] measured the low temperature homogeneity at 350-400 ºC to be MoS_{2+x} ($0 \leq x \leq 0.5$). The extended homogeneity ranges of MoS_2 [98] at low temperature could be attributed to the existence of free sulphur, since free sulphur was found in MoS_3 prepared using the similar approach [99]. However, the present initial thermodynamic calculations indicate that MoS_2 energetically prefers an extended homogeneity at low temperature and the x-ray diffraction experiments from Mering and Levialdi [98] showed clear diffraction patterns. Therefore, the experimental data reported by Mering and Levialdi [98] is also considered as reliable.

The reported melting points of MoS_2 fall in the range of 1185-2375 °C [73, 84, 85, 100, 101]. The experimental methods used [73, 84, 85, 100, 101] were unable to clarify the exact melting point of MoS_2. Cannon [100] estimated the melting point of MoS_2 to be 2375 °C using Tamman's rule. Thermodynamic calculations using the well-established thermodynamic parameters of the gas phase [102] and the MoS_2 compound phase obtained in the present work indicated that the MoS_2 phase will be in equilibrium with gas and pure Mo at 1956 ºC at ambient pressure. Thus, it can be concluded that the melting point of MoS_2 under one bar could not be 2375 °C. The gas pressure attained in the experiments [73, 84, 85, 100] might be much higher than one bar. While the melting temperature or decomposition temperature (1650-1700 ºC) by Zelikman and Belyaevskaya [101] is reasonably at one bar. Starkov and Drobot [77] evaluated the decomposition temperature of MoS_2 to be 1300 ºC and Shang et al. [25] at 1731 ºC. The later one is more reasonable according to the present thermodynamic evaluation.

Vasilyeva et al. [82, 83] interpreted the transition temperature at 1580±15 °C as the boiling temperature of MoS_2. A similar temperature of 1560±10 °C was considered as the polymorphous

transition temperature between α_Mo_2S_3 and β_Mo_2S_3 [73, 84, 85]. In addition, Eremenko et al. [103] also measured "the solidus temperature" to be 1540±15 °C. In consideration of the melting temperature of MoS_2 and the recent experimental data [82, 83], this temperature is more reasonable to be the polymorphous transition temperature of Mo_2S_3.

In addition, Mo_2S_5 [104] and MoS_3 [99, 105-107] can be synthesized by dehydration of their hydrates prepared from thermal decomposition experiments. The preparation of Mo_2S_5 was not further confirmed. And the MoS_3 amorphous [106, 108] is thermally unstable and will decompose to 2H_MoS_2 as temperature increase. The MoS_3 phase cannot be prepared by long time annealing of MoS_2 and S mixtures at 200 and 300 °C [109]. The Mo_3S_4 compound (*Rhombohedral*) was reported to be synthesized by leaching [24, 110] or thermal weight loss of third element of Chevrel phase $Mo_6S_8M_x$ (M=Pb, Sn, Cu, etc.) [111]. According to Flükiger et al. [24], the metastable phase Mo_3S_4 showed superconducting behavior at 1.8 K.

It can be concluded that only Mo_2S_3 and MoS_2 are stable compounds. A summary of the crystal structural information of these compounds is shown in Table 2 in the supplementary data.

3.2.2 The solubility of S in bcc_A2

Straumanis and Shodhan [112] and Schaefer et al. [80] measured the solubilities of S in bcc_A2 (Mo) to be less than 2 at% and 1.49 at%, respectively, at 1100 °C. And Red'ko et al. [97] measured the solubility of S in (Mo) to be larger than 1.86 at% at 1284 °C. These data are consistent.

3.2.3 Other invariant equilibria

The reported eutectic temperatures of Liquid = Mo + Mo_2S_3 are generally consistent as tabulated in Table 3. It is reasonable to identify that the reaction temperature as 1610±12 °C with the liquid composition at about 0.41±0.03 at% S. However, the previous phase diagram evaluations by Brewer and Lamoreaux [75] and Starkov et al. [77] preferred the temperature reported by Eremenko et al. [103]. As discussed before, this temperature is more probably related to the polymorphous transition of Mo_2S_3.

An eutectic reaction Liquid = Mo_2S_3 + MoS_2 at 1953±15 °C was reported by Vasilyeva and Nikolaev [82]. However, the present pre-thermodynamic calculation indicates that gas will always take part in the equilibrium at ambient pressure and such a high temperature.

Moh et al. [73, 84] reported a monotectic reaction, Liquid = Liquid + bcc_A2, at 1950±20 °C with the liquid composition of 5.75 at% S and 38-39.6 at% S. However, the melting point (T_m) of Mo is 2896.00 K, and the enthalpy of fusion ($\Delta_{fus}H$) of Mo is 37479.78 J/mol [113]. The Van't Hoff relationship for initial slopes of the liquidus and solidus is [114]:

$$(dx/dT)_{solidus} - (dx/dT)_{liquidus} = \Delta_{fus}H / RT_m^2 \quad (6)$$

where x is mole fraction, and R is gas constant. Assume there is no sulphur solubility in solid Mo, the initial slope of the liquidus is -0.000538. The calculated limiting slope is shown in Fig. 5. In fact, there is noticeable solid solubility of S in (Mo), the initial slope of liquidus should be even more flat. Assume this monotectic reaction is real, the liquidus in the Mo rich side of the phase diagram would have an even steeper slope than the limiting slope predicted by eq. (6) without considering solid solubility. Thus, the monotectic reaction reported by Moh et al. [73, 84] should not be incorporated in the Mo-S phase diagram.

The dissociation temperatures of MoS_2 and Mo_2S_3 under reduced pressure [27-29, 78, 115-119] were listed in Table 3 in the supplementary data. It can be seen from the table that the dissociation temperatures of MoS_2 and Mo_2S_3 decrease with pressure. This is because equilibrium sulfur pressure decreases as pressure decreases. However, the measurements by Isakova et al. [115] and Srivastava and Avasthi [119] showed very low decomposition temperatures of MoS_2 at ambient pressure which are quite different with the reported melting temperatures or decomposition temperatures as discussed before.

4 Thermodynamic modeling

4.1 Pure elements and stoichiometric compounds

The molar Gibbs energies of Mo, S, α_Mo_2S_3, and β_Mo_2S_3 were described as:

$$^{o}G_i(T) = a + bT + cT\ln T + dT^2 + eT^{-1} + fT^3 + gT^7 + hT^{-9} \quad (7)$$

The Gibbs energies of Mo and S were taken from the SGTE pure element database compiled by Dinsdale [113].

4.2 Liquid and bcc_A2 phases

The molar Gibbs energies of the liquid and bcc_A2 phases were described using regular solution model in the form of Redlich-Kister (R-K) polynomial [120]:

$$^{o}G_m^{\phi} = \sum_{i=1}^{2} x_i\, ^{o}G_i^{\phi} + RT\sum_{i=1}^{2} x_i \ln x_i + \sum_{i=1}^{2}\sum_{j>i}^{2} x_i x_j \sum_{v=0} L_{ij}^{v}(x_i - x_j)^v + \Delta G^{mag} \quad (8)$$

where x_i is the mole fraction of element *i* (*i* = Mo and S), $^{o}G_i^{\phi}$ is the standard molar Gibbs energy of pure element *i* with the ϕ state. L_{ij}^{v} is the binary interaction parameter, and ΔG^{mag} is a term to take into account the effect of magnetic contribution to Gibbs energy [121].

4.3 MoS_2 phase

The molar Gibbs energy of MoS_2 was described using the Compound Energy Formula (CEF) [122]. A two sub-lattice model, $(Mo, S)_1(Mo, S)_2$, was utilized to model the homogeneity range of the MoS_2 phase. The molar Gibbs energy is written as:

$$^{o}G_m = \sum_{i=1}\sum_{j=1} y_i' y_j''\, ^{o}G_{i:j} + RT\sum_{i=1} y_i' \ln y_i' + 2RT\sum_{i=1} y_i'' \ln y_i''$$

$$+\sum_{i=1}\sum_{j>i}\sum_{k=1} y_i^{'} y_j^{'} y_k^{''} \sum_{v=0} (y_i^{'} - y_j^{'})^v L_{ij:k}^v + \sum_{i=1}\sum_{j>i}\sum_{k=1} y_k^{'} y_i^{''} y_j^{''} \sum_{v=0} (y_i^{''} - y_j^{''})^v L_{k:ij}^v \quad (9)$$

where $y_i^{'}$ and $y_i^{''}$ are the site fraction of element *i* in the first and second sub-lattice, respectively. ${}^oG_{i:j}$ is the standard molar Gibbs energy of the hypothetical compound ij_2. $L_{ij:k}^v$ and $L_{k:ij}^v$ are the interaction parameters between *i* and *j* in the first and second sub-lattice, respectively.

4.4 Gas phase

The thermodynamic data of gas was directly taken from the SSUB database [102]. The gas phase was described using the ideal substitutional model. Gas species include Mo, MoS, MoS_2, Mo_2, S, S_2, S_3, S_4, S_5, S_6, S_7, and S_8. The molar Gibbs energy is given as:

$$G_m^o = \sum_{i=1} y_i G_i^o + RT \sum_{i=1} y_i \ln y_i + RT \ln(P/P^o) \quad (10)$$

where G_i^o is the Gibbs energy of gas species *i*, $y_i^{'}$ is the mole fraction of species *i*, *P* is the total pressure, and P^o is the standard pressure, 1 bar.

5 Thermodynamic optimization

The optimization of the thermodynamic parameters was carried out using the ThermoCalc software [123]. It can be seen from section 3 that reliable phase equilibria data and thermodynamic information for the liquid phase are rare. Therefore, Gibbs energies of the solid phases were optimized first. The Gibbs energies of MoS_2 and Mo_2S_3 were evaluated from the thermodynamic property data and phase diagram data. The thermodynamic parameters of the bcc_A2 phase were optimized to reproduce the experimental solubility data. The liquid parameters were only tentatively optimized in the present work, since the reliable phase equilibria data related to the liquid phase is still insufficient. The finally obtained thermodynamic parameters are listed in Table 4.

The calculated heat capacities of MoS_2 and Mo_2S_3 are shown in Fig. 1. The presently calculated heat capacity of MoS_2 excellently reproduces the experimental data as shown in Fig. 1(a). The prediction using Neumann-Kopp rule deviates from the experimental data considerably. A prediction of the heat capacity of Mo_2S_3 was carried out using the heat capacities of pure Mo and MoS_2 instead of pure orthorhombic S. That is $C_P(Mo_2S_3) = 0.5C_P(Mo) + 1.5C_P(MoS_2)$. This is more reasonable than the prediction using Neumann-Kopp rule, since pure orthorhombic S is only stable below 95.15 °C. An alternative way is prediction using first-principles calculations. As shown in Fig. 1(b), the present first-principles calculations results are closer to the presently predicted results using MoS_2 and Mo at low temperature. It should be noted that two sets of Gibbs energies of Mo_2S_3 were optimized based on, respectively, the heat capacity predicted from those of MoS_2 and Mo and heat capacity derived from first-principles calculations. The two sets of Gibbs energies of Mo_2S_3 give similar phase diagram except for the invariant equilibria of liquid = β_Mo_2S_3 + bcc_A2 is with few degree's difference. In the present paper, all the calculations are based on the Gibbs energy derived from the predicted heat capacity using those of MoS_2 and Mo. Fig. 2 shows the calculated heat content of MoS_2. The presently optimized enthalpies and entropies of formation of the Mo-S compounds at 298.15 K are shown in Fig. 3(a) and 3(b), respectively. The reference states for the calculations are bcc_A2 Mo and orthorhombic S. The present model-predicted Gibbs energies of formation of MoS_2 and Mo_2S_3 with respect to bcc_A2 Mo and S_2 (g) reference states are shown in Fig. 4(a) and 4(b), respectively. It can be seen from these diagrams that the present optimization can accurately describe the reliable thermodynamic property data. Fig. 5 shows the calculated *T*-*x* phase diagram of the Mo-S system at 1 bar pressure. The reliable experimental data are reasonably described. The calculated invariant equilibria temperatures from the present work are also shown in Table 3 with acceptable agreement with the experimental data.

6 Thermal decomposition of MoS_2

Thermal decomposition of MoS_2 mineral is one way to produce raw Mo. Fig. 6 shows the calculated *P*-*T* diagrams of Mo_2S_3 (x(S)=0.6) and MoS_2 (x(S)=0.667). The equilibrium states of these two alloys under reduced pressure are presented. The related experimental phase transition temperatures for Mo_2S_3 = Mo (bcc_A2) + gas and MoS_2 = Mo_2S_3 + gas are also appended in the

figures for comparison. Most of the reliable experimental data are reasonably described by the current thermodynamic calculations. It worth noting that the recent data from Wang et al. [27] are accurately described. The decompositions of MoS_2 and Mo_2S_3 are liable to occur at low pressure. As pressure decrease from 10^4 pa to 10^{-3} pa, the dissociation temperature of MoS_2 reduces about 700 K. Similar situation can be seen for Mo_2S_3. MoS_2 will decompose to Mo_2S_3 and then bcc_A2 (raw Mo) as temperature increases under isobar condition.

Fig. 7(a) is the calculated *P*-*x* diagram at 1000 °C. When isothermally reducing pressure, MoS_2 will dissociate to Mo_2S_3 and subsequently to raw Mo. A vacuum of 10^{-2} pa is enough for the formation of raw Mo at this temperature. Further reduction of pressure results in the purification of the raw Mo product by releasing sulphur gas. The effect of temperature on the purification of raw Mo can be seen in Fig. 7(b). High temperature is preferred to lower the sulphur impurity content at isobar condition. At 1500 °C, the required vacuum to produce raw Mo is only about 100 pa, but there is quite amount of sulphur remaining. Thus, it can be concluded that thermal dissociation of MoS_2 is an easy way to produce raw Mo. This process requires controlled pressure and temperature. S_2 as the by product can be condensed. Therefore, this could be an eco-friendly way to manufacture Mo. However, it should be noted that the presence of oxygen and moisture (H_2O) in the reduction process will result in the formation of SO_2 and H_2S.

The kinetics of the decomposition process as one of the additional factors needs to be considered. It is known that the isothermal isobar decomposition of Mo_2S_3 is diffusion controlled [118], while the decomposition of MoS_2 is reaction controlled [27]. The decomposition fraction (*f*) of Mo_2S_3 follows the parabolic equation with time (*t*): $f^2 = k_1 t$ [118], and MoS_2 with a kinetic equation of $1-(1-f)^{1/3} = k_2 t$ [27]. The kinetic parameters k_1 and k_2 are available in refs. [27, 118]. The whole decomposition process at high temperature can be realized within 2 to 3 hours when the conditions are well selected. The outward diffusion of S_2 gas in the Mo shell and the heat transfer from the surroundings to the reaction interface are critical to the decomposition process. Fine mineral particles are beneficial to accelerate the decomposition process of both MoS_2 and Mo_2S_3, since fine particles will decrease the diffusion distance and increase the reaction surface.

7 Summary

The thermodynamic properties, phase equilibria, and phase diagram data in the Mo-S binary system were critically reviewed. First-principles calculations were utilized to resolve the controversial issues related to phase stability and supplement the assessment process. A new Mo-S phase diagram was proposed and optimized. Thermodynamic parameters in the frame of CALPHAD were obtained which can give a reasonable description of the reliable thermodynamic and phase diagram information in the Mo-S system. The calculated pressure-temperature and pressure-composition diagrams indicated that the thermal decomposition of MoS_2 is thermodynamically applicable to the production of raw Mo. The present study showed that pressure and temperature play important roles in controlling the production process and the sulphur content in raw Mo.

References

[1] Z.-f. Cao, H. Zhong, G.-y. Liu, Y.-r. Qiu, S. Wang, Molybdenum extraction from molybdenite concentrate in NaCl electrolyte, J. Taiwan Inst. Chem. Eng., 41 (2010) 338-343.
[2] K. Jiang, Y. Wang, X. Zou, L. Zhang, S. Liu, Extraction of Molybdenum from Molybdenite Concentrates with Hydrometallurgical Processing, JOM, 64 (2012) 1285-1289.
[3] G. Li, Z. You, H. Sun, R. Sun, Z. Peng, Y. Zhang, T. Jiang, Separation of rhenium from lead-rich molybdenite concentrate via hydrochloric acid leaching followed by oxidative roasting, Metals (Basel, Switz.), 6 (2016) 282/281-282/212.
[4] J.D. Lessard, D.G. Gribbin, L.N. Shekhter, Recovery of rhenium from molybdenum and copper concentrates during the Looping Sulfide Oxidation process, Int. J. Refract. Met. Hard Mater., 44 (2014) 1-6.
[5] T.W. Scharf, S.V. Prasad, Solid lubricants: a review, J. Mater. Sci., 48 (2013) 511-531.
[6] H. Li, J. Wang, S. Gao, Q. Chen, L. Peng, K. Liu, X. Wei, Superlubricity between MoS_2 Monolayers, Adv. Mater. (Weinheim, Ger.), 29 (2017) 1701474.
[7] J.-K. Xiao, W. Zhang, L.-M. Liu, L. Zhang, C. Zhang, Tribological behavior of copper-molybdenum disulfide composites, Wear, 384-385 (2017) 61-71.
[8] B. Radisavljevic, A. Radenovic, J. Brivio, V. Giacometti, A. Kis, Single-layer MoS_2 transistors, Nat. Nanotechnol., 6 (2011) 147-150.
[9] A. Verma, W. Jiang, H.H. Abu Safe, W.D. Brown, A.P. Malshe, Tribological behavior of deagglomerated active inorganic nanoparticles for advanced lubrication, Tribol. Trans., 51 (2008) 673-678.
[10] K.F. Mak, K. He, C. Lee, G.H. Lee, J. Hone, T.F. Heinz, J. Shan, Tightly bound trions in monolayer MoS_2, Nat. Mater., 12 (2013) 207-211.
[11] A. Molina-Sanchez, K. Hummer, L. Wirtz, Vibrational and optical properties of MoS_2: from monolayer to bulk, arXiv.org, e-Print Arch., Condens. Matter, (2016) 1-41.

[12] H. Wang, F. Liu, W. Fu, Z. Fang, W. Zhou, Z. Liu, Two-dimensional heterostructures: fabrication, characterization, and application, Nanoscale, 6 (2014) 12250-12272.
[13] L. Xu, W.-Q. Huang, W. Hu, K. Yang, B.-X. Zhou, A. Pan, G.-F. Huang, Two-Dimensional MoS_2 -Graphene-Based Multilayer van der Waals Heterostructures: Enhanced Charge Transfer and Optical Absorption, and Electric-Field Tunable Dirac Point and Band Gap, Chem. Mater., 29 (2017) 5504-5512.
[14] L. Dobusch, S. Schuler, V. Perebeinos, T. Mueller, Thermal Light Emission from Monolayer MoS_2, Adv. Mater. (Weinheim, Ger.), 29 (2017) 1701304.
[15] E.J. Reed, Piezoelectricity: Now in two dimensions, Nat. Nanotechnol., 10 (2015) 106-107.
[16] B. Ouyang, S. Xiong, Z. Yang, Y. Jing, Y. Wang, MoS_2 heterostructure with tunable phase stability: strain induced interlayer covalent bond formation, Nanoscale, 9 (2017) 8126-8132.
[17] Y. Guo, D. Sun, B. Ouyang, A. Raja, J. Song, T.F. Heinz, L.E. Brus, Probing the Dynamics of the Metallic-to-Semiconducting Structural Phase Transformation in MoS_2 Crystals, Nano Lett., 15 (2015) 5081-5088.
[18] B. Ouyang, Z. Mi, J. Song, Bandgap Transition of 2H Transition Metal Dichalcogenides: Predictive Tuning via Inherent Interface Coupling and Strain, J. Phys. Chem. C, 120 (2016) 8927-8935.
[19] Y.-C. Lin, D.O. Dumcenco, Y.-S. Huang, K. Suenaga, Atomic mechanism of the semiconducting-to-metallic phase transition in single-layered MoS_2, Nat. Nanotechnol., 9 (2014) 391-396.
[20] L. Karvonen, A. Saynatjoki, M.J. Huttunen, A. Autere, B. Amirsolaimani, S. Li, R.A. Norwood, N. Peyghambarian, H. Lipsanen, G. Eda, K. Kieu, Z. Sun, Rapid visualization of grain boundaries in monolayer MoS_2 by multiphoton microscopy, Nat. Commun., 8 (2017) 15714.
[21] Y. Wang, T. Yao, J.-L. Yao, J. Zhang, H. Gou, Does the real ReN_2 have the MoS_2 structure?, Phys. Chem. Chem. Phys., 15 (2013) 183-187.
[22] P. Murugan, V. Kumar, Y. Kawazoe, N. Ota, Understanding the Structural Stability of Compound Mo-S Clusters at Sub-Nanometer Level, Mater. Trans., 48 (2007) 658-661.
[23] R.C. Che, N. Bai, L.M. Peng, Structure and growth of monoclinic Mo_2S_3 nanorods, Appl. Phys. Lett., 83 (2003) 3561-3563.
[24] R. Flükiger, R. Baillif, J. Muller, K. Yvon, The constitution diagram of the system copper molybdenum sulfide ($Cu_xMo_6S_8$) in the temperature range 11-2000 K, J. Less-Common Met., 72 (1980) 193-204.
[25] S.-L. Shang, G. Lindwall, Y. Wang, J.M. Redwing, T. Anderson, Z.-K. Liu, Lateral Versus Vertical Growth of Two-Dimensional Layered Transition-Metal Dichalcogenides: Thermodynamic Insight into MoS_2, Nano Lett., 16 (2016) 5742-5750.
[26] F. Liu, Y. Zhou, D. Liu, X. Chen, C. Yang, L. Zhou, Thermodynamic calculations and dynamics simulation on thermal-decomposition reaction of MoS_2 and Mo_2S_3 under vacuum, Vacuum, 139 (2017) 143-152.
[27] L. Wang, P. Guo, J. Pang, L. Luo, P. Zhao, Phase change and kinetics of vacuum decomposition of molybdenite concentrate, Vacuum, 116 (2015) 77-81.
[28] V.V. Sychev, D.Z. Yurchenko, Y.G. Tkachenko, V.A. Obolonchik, S.V. Drozdova, Thermal dissociation of tungsten and molybdenum disulfides; tungsten, molybdenum and niobium diselenides; and boron nitrides in helium, Porosh. Met., 11 (1971) 80-84.
[29] A.V. Gorokh, L.I. Klokotina, K.N. Rispel, Behavior of molybdenite and its dissociation products on heating, Dokl. Akad. Nauk SSSR, 158 (1964) 1183-1185.

[30] S. Cui, I.-H. Jung, Thermodynamic Modeling of the Al-Cr-Mn Ternary System, Metall. Mater. Trans. A, 48 (2017) 1383-1401.
[31] S. Cui, I.-H. Jung, Thermodynamic modeling of the quaternary Al-Cu-Mg-Si system, CALPHAD, 57 (2017) 1-27.
[32] S. Cui, I.-H. Jung, Thermodynamic assessments of the Cr-Si and Al-Cr-Si systems, J. Alloys Compd., 708 (2017) 887-902.
[33] S. Cui, I.-H. Jung, J. Kim, J. Xin, A coupled experimental and thermodynamic study of the Al-Cr and Al-Cr-Mg systems, J. Alloys Compd., 698 (2017) 1038-1057.
[34] S. Cui, L. Zhang, Y. Du, D. Zhao, H. Xu, W. Zhang, S. Liu, Assessment of atomic mobilities in fcc Cu–Ni–Zn alloys, CALPHAD, 35 (2011) 231-241.
[35] S. Cui, Y. Du, L. Zhang, Y. Liu, H. Xu, Assessment of atomic mobilities in fcc Al-Zn and Ni-Zn alloys, CALPHAD, 34 (2010) 446-451.
[36] G. Kresse, J. Furthmüller, Efficiency of ab-initio total energy calculations for metals and semiconductors using a plane-wave basis set, Comp. Mater. Sci., 6 (1996) 15-50.
[37] G. Kresse, J. Furthmüller, Efficient iterative schemes for ab initio total-energy calculations using a plane-wave basis set, Phys. Rev. B, 54 (1996) 11169-11186.
[38] G. Kresse, D. Joubert, From ultrasoft pseudopotentials to the projector augmented-wave method, Phys. Rev. B, 59 (1999) 1758-1775.
[39] P.E. Blöchl, Projector augmented-wave method, Phys. Rev. B, 50 (1994) 17953-17979.
[40] J.P. Perdew, K. Burke, M. Ernzerhof, Generalized Gradient Approximation Made Simple, Phys. Rev. Lett., 77 (1996) 3865.
[41] H.J. Monkhorst, J.D. Pack, Special points for Brillouin-zone integrations, Phys. Rev. B, 13 (1976) 5188-5192.
[42] P.E. Blöchl, O. Jepsen, O.K. Andersen, Improved tetrahedron method for Brillouin-zone integrations, Phys. Rev. B, 49 (1994) 16223-16233
[43] A. Togo, L. Chaput, I. Tanaka, G. Hug, First-principles phonon calculations of thermal expansion in Ti_3SiC_2, Ti_3AlC_2, and Ti_3GeC_2, Phys. Rev. B, 81 (2010) 174301.
[44] A. Togo, F. Oba, I. Tanaka, First-principles calculations of the ferroelastic transition between rutile-type and CaC_2-type SiO_2 at high pressures, Phys. Rev. B, 78 (2008) 134106.
[45] C.T. Anderson, The heat capacities of molybdenite and pyrite at low temperatures, J. Am. Chem. Soc., 59 (1937) 486-487.
[46] D.F. Smith, D. Brown, A.S. Dworkin, D.J. Sasmor, E.R. Van Artsdalen, Low-temperature heat capacity and entropy of molybdenum trioxide and molybdenum disulfide, J. Am. Chem. Soc., 78 (1956) 1533-1536.
[47] H.L. Kiwia, E.F. Westrum, Low-temperature heat capacities of molybdenum diselenide and ditelluride, J. Chem. Thermodyn., 7 (1975) 683-691.
[48] J.J. McBride, E.F. Westrum, Low-temperature heat capacity of anisotropic crystals lamellar molybdenum disulfide, J. Chem. Thermodyn., 8 (1976) 37-44.
[49] D.R. Fredrickson, M.G. Chasanov, Enthalpy of molybdenum disulfide to 1200 K by drop calorimetry, J. Chem. Thermodyn., 3 (1971) 693-696.
[50] L.S. Volovik, L.N. Bazhenova, A.S. Bolgar, L.A. Klochkov, S.V. Drozdova, V.F. Primachenko, I.I. Timofeeva, Thermodynamic properties of transition metal sulfides, Izv. Akad. Nauk SSSR, Neorg. Mater., 15 (1979) 638-642.
[51] L.S. Volovik, V.V. Fesenko, A.S. Bolgar, S.V. Drozdova, L.A. Klochkov, V.F. Primachenko, Enthalpy and heat capacity of molybdenum disulfide, Poroshk. Metall. (Kiev), (1978) 54-59.

[52] J. Yuan, Z. Lv, Q. Lu, Y. Cheng, X. Chen, L. Cai, First-principles study of the phonon vibrational spectra and thermal properties of hexagonal MoS_2, Solid State Sci., 40 (2015) 1-6.
[53] K. Ali, Y. Haluk, K. Alper, Ç. Tahir, S. Cem, Thermal transport properties of MoS_2 and $MoSe_2$ monolayers, Nanotechnology, 27 (2016) 055703.
[54] E.F. Westrum, J.J. McBride, Temperature dependence of heat capacity of Molybdenite, Bull. Am. Phys. Soc., 29 (1954) 22.
[55] I.A. Makolkin, Free energy and the heat of formation of molybdenum disulfide from measurements of the electromotive forces, Zh. Fiz. Khim., 14 (1940) 110-112.
[56] J.P. Hager, J.F. Elliott, The free energies of formation of CrS, Mo_2S_3, and WS_2, Trans. Am. Inst. Min., Metall. Pet. Eng., 239 (1967) 513-520.
[57] P.A.G. O'Hare, E. Benn, F.Y. Cheng, G. Kuzmycz, Fluorine bomb calorimetric study of molybdenum disulfide. Standard enthalpies of formation of the di- and sesquisulfides of molybdenum, J. Chem. Thermodyn., 2 (1970) 797-804.
[58] P.A.G. O'Hare, B.M. Lewis, B.A. Parkinson, Standard molar enthalpy of formation by fluorine-combustion calorimetry of tungsten diselenide (WSe_2). Thermodynamics of the high-temperature vaporization of tungsten diselenide. Revised value of the standard molar enthalpy of formation of molybdenite (MoS_2), J. Chem. Thermodyn., 20 (1988) 681-691.
[59] I.S. Sukhushina, I.A. Vasil'eva, Thermodynamic properties of molybdenite, Geokhimiya, (1990) 1063-1068.
[60] L. Bartovská, C. Černý, Chemical equilibria in heterogeneous systems. Part X. The influence of the structure of molybdenum disulfide on its reactivity, Collect. Czech. Chem. Commun., 52 (1987) 678-685.
[61] S.C. Schaefer, Electrochemical determination of Gibbs energies of formation of molybdenum disulfide and tungsten disulfide, in, Bur. Mines, 1980, pp. 17 pp.
[62] S.C. Schaefer, N.A. Gokcen, Electrochemical determination of thermodynamic properties of molybdenite (MoS_2), High Temp. Sci., 12 (1980) 267-276.
[63] J.R. Stubbles, F.D. Richardson, Equilibriums in the system molybdenum + sulfur + hydrogen, Trans. Faraday Soc., 56 (1960) 1460-1466.
[64] Y. Pan, W. Guan, Effect of sulfur concentration on structural, elastic and electronic properties of molybdenum sulfides from first-principles, Int. J. Hydrogen Energy, 41 (2016) 11033-11041.
[65] G. Pouillard, P. Perrot, Free enthalpy of formation and region of stability of molybdenum(III) and molybdenum(IV) sulfide, C. R. Hebd. Seances Acad. Sci., Ser. C, 281 (1975) 143-146.
[66] H.R. Larson, J.F. Elliott, Standard free energy of formation of certain sulfides of some transition elements and zinc, Trans. Am. Inst. Min., Metall. Pet. Eng., 239 (1967) 1713-1720.
[67] Y. Suzuki, T. Uchida, M. Wakihara, M. Taniguchi, Phase relationship in molybdenum-sulfur system at high temperatures, Mater. Res. Bull., 16 (1981) 1085-1090.
[68] A.N. Zelikman, O.E. Krein, Thermal dissociation of molybdenum disulfide, Zh. Fiz. Khim., 29 (1955) 2081-2085.
[69] N. Parravano, G. Malquori, Researches on molybdenum sulfides. II. Equilibrium of reduction of molybdenum bisulfide by means of hydrogen, Alli accad. Lincei [6], 7 (1928) 109-112.
[70] N. Parravano, G. Malquori, Researches on molybdenum sulfides. I. The vapor pressures of the sulfur of molybdenum trisulfide, Alli accad. Lincei [6], 7 (1928) 19-22.
[71] R.A. Isakova, Vapor and dissociation pressures of molybdenite, Izvest. Akad. Nauk Kazakh. S.S.R., Ser. Met., Obogashchen. i Ogneuporov, No. 3 (1961) 3-10.
[72] C.L. McCabe, Sulfur pressure measurements of molybdenum sesquisulfide in equilibrium with molybdenum, J. Met., 7 (1955) 61-63.

[73] S. Takeno, G.H. Moh, Liquidus reactions of the Mo-S system, Neues Jahrb. Mineral., 131 (1977) 43-48.
[74] G.H. Moh, High-temperature metal sulfide chemistry, in: Topics in Current Chemistry: Aspects of Molybdenum and Related Chemistry, Springer Berlin Heidelberg, Berlin, Heidelberg, 1978, pp. 107-151.
[75] L. Brewer, R.H. Lamoreaux, Mo-S, Bull. Alloy Phase Diagrams, 93 (1980) 93-95.
[76] W.B. Johnson, W.S. Hong, D.W. Readey, A molybdenum-sulfur binary phase diagram, Scr. Metall., 17 (1983) 919-922.
[77] V.V. Starkov, D.V. Drobot, E.A. Pisarev, A.N. Zelikman, The molybdenum-sulfur system, Izv. Vyssh. Uchebn. Zaved., Tsvetn. Metall., (1987) 51-57.
[78] A.V. Gorokh, L.N. Rusakov, A.A. Savinskaya, Synthesis and characteristics of molybdenum sesquisulfide, Dokl. Akad. Nauk SSSR, 156 (1964) 541-542.
[79] N. Morimoto, G. Kullerud, Ore minerals. The Mo-S system, Year Book - Carnegie Institution of Washington, 1961 (1962) 143-144.
[80] S.C. Schaefer, A.H. Larson, A.W. Schlechten, Sulfur pressure variation of molybdenum disulfide at 1100 °C, Trans. Am. Inst. Min., Metall. Pet. Eng., 230 (1964) 594-595.
[81] G. Krabbes, H. Oppermann, J. Henke, Chemischer Transport und thermische Stabilität von Sulfidphasen des Molybdäns, Z. Anorg. Allg. Chem., 470 (1980) 7-17.
[82] I.G. Vasilyeva, R.E. Nikolaev, High-temperature solid-vapor and liquid-vapor transitions in binary and ternary chalcogenides La_2S_3, MoS_2, Mo_2S_3 and $LiInSe_2$, J. Alloys Compd., 452 (2008) 89-93.
[83] Y.I. Gibner, I.G. Vasilyeva, Rapid Heating in High-Temperature Thermomicroscopic Analysis, J. Therm. Anal. Calorim., 53 (1998) 151-160.
[84] G.H. Moh, G. Udubasa, R. Hueller, High temperature phase equilibriums in the molybdenum-sulfur system, Metall (Isernhagen, Germany), 28 (1974) 804.
[85] G.H. Moh, High-temperature metal sulfide chemistry, (1978).
[86] Y. Han, Molybdenite polytypes and mechanism of polytype formation, Diqiu Kexue, 13 (1988) 385-394.
[87] L.A. Arutyunyan, E.K. Khurshudyan, Synthesis of molybdenum disulfide from thiomolybdate solutions at elevated temperature, Geokhimiya, (1966) 650-658.
[88] A.N. Zelikman, Y.D. Christyakov, G.V. Indenbaum, O.E. Krein, Crystal structure of molybdenum disulfide prepared by different methods, Kristallografiya, 6 (1961) 389-394.
[89] A.N. Zelikman, G.V. Indenbaum, M.V. Teslitskaya, V.P. Shalankova, Structural transformations of synthetic molybdenum disulfide, Kristallografiya, 14 (1969) 795-799.
[90] M.O. Rikel, Z.M. Alekseeva, Phase relations in the lead-molybdenum-sulfur system in the 900-1150 °C and 13.3-266 gPa ranges, Izv. Akad. Nauk SSSR, Neorg. Mater., 17 (1981) 2089-2094.
[91] A.H. Clark, Compositional differences between hexagonal and rhombohedral molybdenite, Neues Jahrb. Mineral., Monatsh., (1970) 33-38.
[92] R.J.J. Newberry, Polytypism in molybdenite (I): a non-equilibrium impurity-induced phenomenon, Am. Mineral., 64 (1979) 758-767.
[93] R.J.J. Newberry, Polytypism in molybdenite (II): relationships between polytypism, ore deposition/alteration stages and rhenium contents, Am. Mineral., 64 (1979) 768-775.
[94] H. Rau, Estimation of the homogeneity range of molybdenum disulfide, J. Phys. Chem. Solids, 41 (1980) 765-767.

[95] S. Yamamoto, M. Wakihara, M. Taniguchi, Phase relations in the lead-molybdenum-sulfur ternary system at 1000 °C and the superconductivity of lead molybdenum sulfide ($Pb_xMo_6S_{8-y}$), Mater. Res. Bull., 20 (1985) 1493-1500.
[96] L.E. Ugryumova, V.A. Snurnikova, R.A. Isakova, V.P. Bystrov, A.V. Vanyukov, I.A. Sapukov, Molybdenum disulfide dissociation pressure, Zh. Prikl. Khim. (Leningrad), 51 (1978) 2684-2687.
[97] A.I. Red'ko, V.A. Spitsyn, L.E. Ugryumova, I.A. Sapukov, R.A. Isakova, Phase equilibrium in the molybdenum-sulfur system, Izv. Akad. Nauk Kaz. SSR, Ser. Khim., (1982) 10-15.
[98] J. Mering, A. Levialdi, Molybdenum sulfides, Compt. rend., 213 (1941) 798-800.
[99] E.Y. Rode, B.A. Lebedev, Physicochemical study of molybdenum trisulfide and products of its thermal decomposition, Zh. Neorg. Khim., 6 (1961) 1189-1203.
[100] P. Cannon, Melting point and sublimation of molybdenum disulfide, Nature (London, U. K.), 183 (1959) 1612-1613.
[101] A.N. Zelikman, L.V. Belyaevskaya, The melting point of molybdenite, Zh. Neorg. Khim., 1 (1956) 2239-2244.
[102] http://www.thermocalc.com/products-services/databases/thermodynamic/.
[103] V.N. Eremenko, V.E. Listovnichii, A.A. Opalovskii, V.E. Fedorov, Physicochemical study of the molybdenum-sulfur system, Khal'kogenidy, No. 2 (1970) 92-97.
[104] F. Mawrow, M. Nokolow, New sulfides of molybdenum, Z. Anorg. Allg. Chem., 95 (1916) 188-193.
[105] D.E. Wilcox, L.A. Bromley, Computer estimation of heat and free energy of formation for simple inorganic compounds, Ind. Eng. Chem., 55 (1963) 32-39.
[106] P. Ratnasamy, L. Rodrique, A.J. Leonard, Structural and textural studies in molybdenum sulfide systems, J. Phys. Chem., 77 (1973) 2242-2245.
[107] M.I. Ermolaev, S.M. Basitova, N.A. Shatkovskaya, DTA and differential thermogravimetric analysis of rhenium and molybdenum sulfides, Dokl. Akad. Nauk Tadzh. SSR, 18 (1975) 27-29.
[108] J.C. Wildervanck, F. Jellinek, Preparation and crystallinity of molybdenum and tungsten sulfides, Z. Anorg. Allg. Chem., 328 (1964) 309-318.
[109] M. Stemprok, Bismuth-molybdenum-sulfur system, Year Book - Carnegie Institution of Washington, 65 (1967) 336-337.
[110] R. Chevrel, M. Sergent, J. Prigent, New molybdenum sulfide, Mo_3S_4. Preparation, properties, and crystal structure, Mater. Res. Bull., 9 (1974) 1487-1498.
[111] R. Flükiger, H. Devantay, J. Jorda, J. Muller, Metallurgical and physical properties of ternary Molybdenum Sulfides ($M_xMo_3S_4$) as synthetized in the bulk state, IEEE Trans. Magn.,13 (1977) 818-820.
[112] M.E. Straumanis, R.P. Shodhan, Lattice constants, thermal expansion coefficients, and densities of molybdenum and the solubility of sulfur, selenium, and tellurium in it at 1100 °C, Z. Metallk., 59 (1968) 492-495.
[113] A.T. Dinsdale, SGTE data for pure elements, CALPHAD, 15 (1991) 317-425.
[114] H. Okamoto, T.B. Massalski, Thermodynamically Improbable Phase Diagrams, J. Phase Equilib., 12 (1991) 148-168.
[115] R.A. Isakova, L.E. Ugryumova, K.S. Amosova, N.A. Potanina, Behavior of molybdenum disulfide during heating in vacuo, Izv. Akad. Nauk Kaz. SSR, Ser. Khim., 23 (1973) 6-10.
[116] A.A. Opalovskii, V.E. Fedorov, Thermal dissociation of molybdenum disulfide in vacuum, Dokl. Akad. Nauk SSSR, 163 (1965) 900-901.

[117] V.L. Kalikhman, S.V. Radzikovskaya, V.F. Bukhanevich, E.P. Gladchenko, In vacuo behavior of tungsten, molybdenum, niobium, and tantalum sulfides, Porosh. Met., 10 (1970) 55-60.
[118] Y. Maru, H. Yoshida, Y. Kondo, On the Thermal Decomposition Rate of Molybdenum Sesquisulphide (Mo_2S_3) in Vacuum, Trans. Jpn. Inst. Met., 10 (1969) 8-11.
[119] S.K. Srivastava, B.N. Avasthi, High pressure synthesis and characterization of molybdenum disulfide, J. Less-Common Met., 124 (1986) 85-92.
[120] O. Redlich, A.T. Kister, Thermodynamics of nonelectrolytic solutions. Algebraic representation of thermodynamic properties and the classification of solutions, Ind. Eng. Chem. Res., 40 (1948) 84,85-88.
[121] M. Hillert, M. Jarl, A model for alloying effects in ferromagnetic metals, CALPHAD, 2 (1978) 227-238.
[122] B. Sundman, J. Ågren, A regular solution model for phases with several components and sublattices, suitable for computer applications, J. Phys. Chem. Solids, 42 (1981) 297-301.
[123] http://www.thermocalc.com.
[124] M.C.L. Patterson, L.J.R. Cohen, J.A. Charles, Studies in the system molybdenum-sulfur, Trans. - Inst. Min. Metall., Sect. C, 96 (1987) C98-C102.

Table Captions

Table 1 Summary of thermodynamic studies in the Mo-S system.

Table 2 Summary of phase diagram studies in the Mo-S system.

Table 3 Summary of invariant reactions in the Mo-S system.

Table 4 Summary of thermodynamic parameters for the Mo-S system (in J mol^{-1} or J mol^{-1} K^{-1}).

Figure Captions

Fig. 1 Calculated heat capacities of (a) MoS_2 and (b) Mo_2S_3 along with the experimental data.

Fig. 2 Calculated heat content of MoS_2 along with the experimental data.

Fig. 3 Calculated (a) enthalpies of formation and (b) entropies of formation of compounds in the Mo-S system at 298.15 K along with the experimental data.

Fig. 4 Calculated Gibbs energies of formation of (a) MoS_2 and (b) Mo_2S_3 along with the experimental data.

Fig. 5 Calculated Mo-S phase diagram at 1 bar along with the experimental data.

Fig. 6 Calculated pressure-temperature (*P*-*T*) diagrams along with the experimental data. (a) $x(S) = 0.6$, the experimental data are for Mo_2S_3 = bcc_A2 + gas. (b) $x(S) = 0.667$, the experimental data are for $MoS_2 = Mo_2S_3$ + gas.

Fig. 7 Calculated pressure-composition (*P*-*x*) diagrams along with the experimental data. (a) 1000 °C, (b) 1000-1500 °C (in logarithm composition scale).

Table 1 Summary of thermodynamic studies in the Mo-S system.

Type of experimental data	Experimental details	Ref.
Heat capacity of 2H_MoS_2	56-292 K, adiabatic calorimetry	[45]
	20-100 K, low temperature adiabatic calorimetry	[46]
	6-212 K, adiabatic calorimetry	[47]
	5-350 K, adiabatic calorimetry	[48]
	525-1205 K, calorimetry	[49]
	773-1973 K, vacuum calorimetry	[50, 51]
Heat content of 2H_MoS_2	525-1205 K, calorimetry	[49]
	773-1973 K, vacuum calorimetry	[50, 51]
Entropy of 2H_MoS_2	298.15 K, 63.18±0.84 J/mol-K, adiabatic calorimetry	[45]
	298.15 K, 65.04 J/mol-K, emf	[55]
	298.15 K, 62.43±0.08 J/mol-K, adiabatic calorimetry	[54]
	298.15 K, 62.59 J/mol-K	[49]
	298.15 K, 62.59±0.08 J/mol-K, adiabatic calorimetry	[48]
	298.15 K, 62.59 J/mol-K	[50, 51]
Entropy	298.15 K, Mo_2S_3 (124.26 J/mol-K), MoS (52.72 J/mol-K), 2H_MoS_2 (71.54 J/mol-K), estimation	[56]
Entropy of α_Mo_2S_3	298.15 K, 115.53 J/mol-K, first-principles	This work
Formation enthalpy of 2H_MoS_2	298.15 K, -78003.71 J/g-atoms, emf at 15, 25, and 35 °C, Pt|H_2|KCl(0.01N)||KCl(0.01N)|H_2S|MoS_2	[55]
	298.15 K, -91266.67±500 J/g-atoms, fluorine bomb calorimetry	[57, 58]
	298.15 K, -92702.10±697 J/g-atoms, estimation	[61, 62]
	298.15 K, -91066.67 J/g-atoms, estimation	[60]
	298.15 K, -81966.67±1667 J/g-atoms, evaluation	[59]
	0 K, -94529.85 J/g-atoms, first-principles; 298.15 K, -91699.42 J/g-atoms, Calphad	This work
Formation enthalpy of 2H_Mo_3	0 K, 137038.24 J/g-atoms, first-principles; 298.15 K, 24666.67 J/g-atoms, Calphad	This work
Formation enthalpy of 2H_S_3	0 K, 71112.47 J/g-atoms, first-principles; 298.15 K, 18333.33 J/g-atoms, Calphad	This work

Formation enthalpy of 2H_Mo_2S	0 K, 28421.14 J/g-atoms, first-principles; 298.15 K, 134699.42 J/g-atoms, Calphad	This work
Formation enthalpy of 3R_MoS_2	0 K, -94500.35 J/g-atoms, first-principles	This work
Formation enthalpy of α_Mo_2S_3	298.15 K, -81169.60±2510 J/g-atoms, estimation	[57]
	0 K, -76317.17 J/g-atoms, first-principles; 298.15 K, -79423.68 J/g-atoms, Calphad [a]; 298.15 K, -76614.904 J/g-atoms, Calphad [b]	This work
Formation enthalpy of Mo_3S_4	0 K, -75601.84 J/g-atoms, first-principles	This work
Formation Gibbs energy of 2H_MoS_2	1073-1373 K, MoS_2-H_2-H_2S-Mo equilibrium	[69, 70]
	1073-1373 K, MoS_2-H_2-H_2S-Mo equilibrium	[68]
	1119-1473 K, molybdenum sulphides-H_2-H_2S-Mo equilibrium, a radiochemical method, chemical analysis, X-ray diffraction analysis	[63]
	1738-1523 K, dissociation pressure measurements	[71]
	1123-1373 K, emf, MoO_2 (c), MoS_2 (c), Pt, P(SO_2)=1atm, PO_2|O^{2-}, $Zr_{0.85}Ca_{0.15}O_{1.85}$| P($O_2$)=1atm, Pt	[66]
	1033-1273 K, MoS_2-H_2S-H_2-Mo equilibrium	[65]
	867-1209 K, emf, Pt, MoS_2, MoO_2, SO_2=1 atm|ZrO_2|O_2=0.0112 atm, Pt	[61, 62]
	1223 K, S(gas)-MoS_2-Mo equilibrium, MoS_2-H_2S-H_2-Mo equilibrium	[67]
	569.4-1276.8 K, MoS_2-H_2S-H_2-Mo equilibrium	[60]
	1100-1370 K, emf, Pt|Fe, $Fe_{0.95}O$|0.85ZrO_2-0.15Y_2O_3|$MoS_{1.457}$, MoS_2, MoO_2|Pt	[59]
Formation Gibbs energy of Mo_2S_3	1300-1425 K, Knudsen effusion method	[72]
	1119-1473 K, molybdenum sulphides-H_2-H_2S-Mo equilibrium, a radiochemical method, chemical analysis, X-ray diffraction analysis	[63]
	1365-1610 K, MoS_2-H_2S-H_2-Mo equilibrium	[56]
	1033-1273 K, MoS_2-H_2S-H_2-Mo equilibrium	[65]
	1223 K, S(gas)-MoS_2-Mo equilibrium, MoS_2-H_2S-H_2-Mo equilibrium	[67]
	1100-1373 K, evaluation	[59]

[a] heat capacity predicted from MoS_2 and Mo; [b] heat capacity calculated from first-principles calculations.

Table 2 Summary of phase diagram studies in the Mo-S system.

Type of experimental data	Experimental details [a]	Ref.
Solubility of S in (Mo)	1.49 at% S at 1100 °C, CA	[80]
	<2 at% S at 1100 °C, LPM	[112]
	>1.86 at% S at 1284 °C, MSA	[97]
Homogeneity of Mo_2S_3	$Mo_{2.06}S_3$ at 700-935 °C, QE, MA, XRD	[79]
	$MoS_{1.457}$ at 950 °C, solid-gas reaction under varying sulfur pressure, XRD	[67]
	$Mo_2S_{3-\delta}$ ($0.008 \leq \delta \leq 0.036$), CTR	[81]
Homogeneity of MoS_2	MoS_2 at 800-1000 °C, $MoS_{2.5}$ at 350-400 °C, (MoS_{2+x} ($0 \leq x \leq 0.5$)), thermal decomposition of $(NH_4)_3PMo_{12}O_{40}$, XRD, DM	[98]
	MoS_2, QE, MA, XRD	[79]
	66.6(9)-69.09 at% S at 1100 °C, equilibration of Mo/S(g) and $MoS_{1.99}$/S(g)	[80]
	66.74-66.78 at% S in the S side at 840-1025 ºC, XRD	[96]
	MoS_2 at 900-1100 °C, S(g)-H_2-MoS_2 equilibrium	[94]
	$MoS_{1.978}$ to MoS_2 (66.52-66.67 at%) at 950 °C, $MoS_{1.983}$ to MoS_2 (66.48-66.67 at%) at 750 °C, solid-gas reaction under varying sulfur pressure, XRD	[67]
	$MoS_{1.85\pm0.05}$-$MoS_{1.9}$ (64.91-65.52 at%) at 900-1284 °C, XRD, MSA, equilibration, CA, MIA	[97]
	$MoS_{1.97}$ (66.33 at% S) at 1000 °C, TGA	[95]
Phase diagram	up to 66.67 at% S, QE, MA, XRD	[79]
	up to 52.53 at% S, TA, MA, DIL, CA, XRD	[103]
	up to 66.67 at% S and 500-1900 °C, DTA, QE	[84]
	up to 66.7 at% S, evaluation, DTA, QE, MA	[73]
	Invariant phase equilibria, TMA	[83]
	35-66.7 at% S, TMA, AAET, DDM	[82]

[a] CA = Chemical Analysis; LPM = Lattice Parameters Measurements; MSA = Mass Spectrometry Analysis; QE = Quenching Experiments; MA = Microscopic Analysis; XRD = X-Ray Diffraction analysis; CTR = Chemical Transportation Reaction; DM = Density Measurements; MIA = MIneralogical Analysis; TGA = Thermal Gravity Analysis; TA = Thermal Analysis; DIL = DILatometric analysis; DTA = Differential Thermal Analysis; TMA = high heating rate Thermo-Microscopic Analysis; AAET = Analytical Atomic-Emission Technique; DDM = Differential Dissolution Method.

Table 3 Summary of invariant reactions in the Mo-S system.

Reaction (at% S)	Temperature °C	Method [a]	Ref.
Melting point of MoS_2			
	2375, >1800±20	TR, TA, WLM	[100]
	1650-1700 (incongruent)	TGA, TA, MA, CA, XRD	[101]
	~1900	DTA, MA	[84]
	~>2100	DTA, MA	[73]
	>2000	DTA, MA	[85]
	1731	Calphad	[25]
Boiling point of MoS_2			
	1565	TA (10^{-5}-10^{-4} atm)	[71]
	1575	TA, MA	[83]
	1580±15	TA, MA, AAET, DDM	[82]
Liquid = β_Mo_2S_3 + gas			
0.61	1754	Calphad	This work
MoS_2 = β_Mo_2S_3 + gas			
	1719	Calphad	This work
Melting point of β_Mo_2S_3			
	1740±10 (incongruent)	DTA, MA	[84]
	1600 (dissociation)	TA	[78]
	1740 (congruent)	TA, MA	[83]
	1780±10 (congruent)	TA, MA, AAET, DDM	[82]
	<1700 (incongruent)	DTA, MA	[73]
	<1700 (incongruent)		[85]
	1740±10 (incongruent)		[76]
	1600 (incongruent)		[77]
	1753 (congruent)	Calphad	[25]
	1754.2 (congruent)	Calphad	This work
Liquid = Mo + β_Mo_2S_3			
0.37	1607±12	DTA, MA	[84]
	1645	TA, MA	[83]
0.44	1615±15	TA, MA, AAET, DDM	[82]
0.41	1610±10	DTA, MA	[73]
0.48±1	~1460	MA	[124]
0.37	1607±12		[76]
0.41	1610±15	DTA, MA	[85]
	1540±15	TA, MA, DIL, CA, XRD	[103]
0.42	1550±100	Calphad	[75]
	1540		[77]
	1609	Calphad	[25]
0.445	1616	Calphad	This work
Liquid = MoS_2 + Mo_2S_3			
	1953±15	TA, MA, AAET, DDM	[82]
	1731	Calphad	[25]
Liquid = Liquid + bcc_A2			
	1950±20	DTA, MA	[73]
	~1950		[85]

α_Mo_2S_3 = Mo + MoS_2			
	610±5	DTA, MA	[84]
	610±5	MA, XRD	[79]
	664	Extrapolated	[65]
	664±50	Calphad	[75]
	610±5		[76]
	610		[77]
	629	Calphad	[25]
	610	Calphad	This work
S_2 (g) + Liquid = MoS_2			
	1750±50	Calphad	[75]
	1731	Calphad	[25]
S_2 (g) = Liquid + MoS_2			
	444.6	Calphad	[75]
	444		[77]
	461	Calphad	[25]
	461	Calphad	This work
3R_MoS_2 = 2H_MoS_2			
	1000		[76]
α_Mo_2S_3 = β_Mo_2S_3			
	1560±10	DTA, MA	[84]
	1560±10	DTA, MA	[73]
	1560		[85]
	1560	Calphad	This work

[a] TR = Tammann's Rule; TA = Thermal Analysis; WLM = Weight Loss Measurement; TGA = Thermal Gravity Analysis; DTA = Differential Thermal Analysis; MA = Microscopic Analysis; CA = Chemical Analysis; AAET = Analytical Atomic-Emission Technique, DDM = Differential Dissolution Method, DIL = DILatometric analysis.

Table 4 Summary of thermodynamic parameters for the Mo-S system (in J mol^{-1} or J mol^{-1} K^{-1}).

Phase	Thermodynamic parameters	Ref.
Gas	$(Mo, MoS, MoS_2, Mo_2, S, S_2, S_3, S_4, S_5, S_6, S_7, S_8)_1$	
	${}^oG_{Mo} = {}^oG_{Mo}^{gas}$	[102]
	${}^oG_{MoS} = {}^oG_{MoS}^{gas}$	[102]
	${}^oG_{MoS_2} = {}^oG_{MoS_2}^{gas}$	[102]
	${}^oG_{Mo_2} = {}^oG_{Mo_2}^{gas}$	[102]
	${}^oG_{S} = {}^oG_{S}^{gas}$	[102]
	${}^oG_{S_2} = {}^oG_{S_2}^{gas}$	[102]
	${}^oG_{S_3} = {}^oG_{S_3}^{gas}$	[102]
	${}^oG_{S_4} = {}^oG_{S_4}^{gas}$	[102]
	${}^oG_{S_5} = {}^oG_{S_5}^{gas}$	[102]
	${}^oG_{S_6} = {}^oG_{S_6}^{gas}$	[102]
	${}^oG_{S_7} = {}^oG_{S_7}^{gas}$	[102]
	${}^oG_{S_8} = {}^oG_{S_8}^{gas}$	[102]
Liquid	$(Mo, S)_1$	
	${}^oG_{Mo} = {}^oG_{Mo}^{liq}$	[113]
	${}^oG_{S} = {}^oG_{S}^{liq}$	[113]
	$L_{Mo,S}^0 = -166033.05 + 2.11T$	This work
	$L_{Mo,S}^1 = 38149.91 + 40.00T$	This work
	$L_{Mo,S}^2 = 43472.76 - 30.73T$	This work
bcc_A2	$(Mo, S)_1(Va)_3$	
	${}^oG_{Mo} = {}^oG_{Mo}^{bcc}$	[113]

	$^{o}G_{S}=^{o}G_{S}^{bcc}$	[113]
	$L_{Mo,S}^{0}=-225000+32.50T$	This work
α_Mo_2S_3	$(Mo_2S_3)_1$	
	$^{o}G_{\alpha\_Mo2S3}=-439761.4+714.875T-124.08373T\ln T$ $+820846.46\,T^{-1}-7.1208711\times10^{-4}T^{2}-1.46894988\times10^{-6}T^{3}$	This work [a]
	$^{o}G_{\alpha\_Mo2S3}=-422200.0+642.312T-116.44538T\ln T$ $+646849.415\,T^{-1}-7.36469482\,5\times10^{-4}T^{2}-5.14552535\times10^{-8}T^{3}$	This work [b]
β_Mo_2S_3	$(Mo_2S_3)_1$	
	$^{o}G_{\beta\_Mo2S3}=^{o}G_{\alpha\_Mo2S3}+1833-T$	This work
MoS_2	$(Mo, S)_1(Mo, S)_2$	
	$^{o}G_{Mo:Mo}=74000.00-8T+3^{o}G_{Mo}^{bcc}$	This work
	$^{o}G_{S:S}=55000-30T+3^{o}G_{S}^{ort}$	This work
	$^{o}G_{Mo:S}=-300558.04+437.80T-73.785239T\ln T$ $+500962.593\,T^{-1}-6.28908896\times10^{-4}T^{2}-8.24179085\times10^{-7}T^{3}$	This work
	$^{o}G_{S:Mo}=^{o}G_{Mo:Mo}+^{o}G_{S:S}-^{o}G_{Mo:S}$	This work
	$L_{Mo,S:S}^{0}=-43000$	This work
	$L_{MoMo,S}^{0}=-28000$	This work
	$L_{MoMo,S}^{1}=-22000$	This work
Monoclinic	$(S)_1$	
	$^{o}G=^{o}G_{S}^{mon}$	[113]
Orthorhombic	$(S)_1$	
	$^{o}G=^{o}G_{S}^{ort}$	[113]

[a] heat capacity predicted from MoS_2 and Mo; [b] heat capacity calculated from first-principles calculations.

Figures

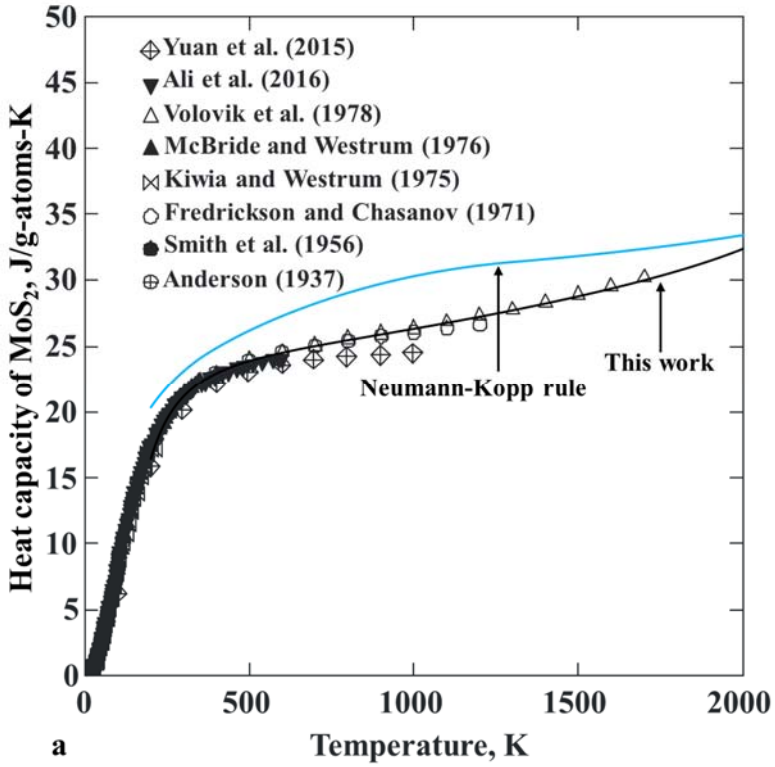
Yuan et al. (2015)
Ali et al. (2016)
Volovik et al. (1978)
McBride and Westrum (1976)
Kiwia and Westrum (1975)
Fredrickson and Chasanov (1971)
Smith et al. (1956)
Anderson (1937)
Neumann-Kopp rule
This work
Heat capacity of MoS2, J/g-atoms-K
Temperature, K
a

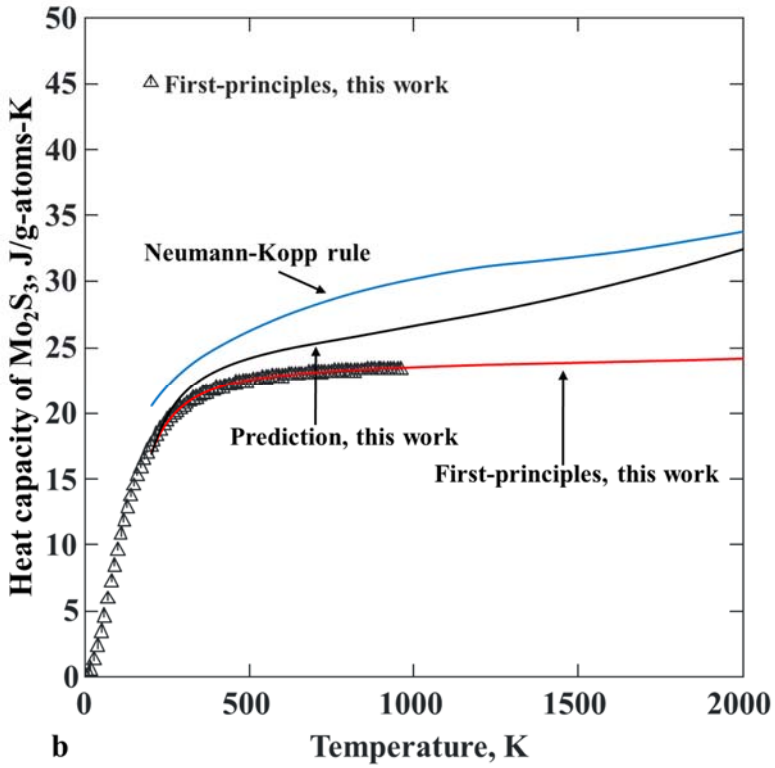
First-principles, this work
Neumann-Kopp rule
Prediction, this work
First-principles, this work
Heat capacity of Mo2S3, J/g-atoms-K
Temperature, K
b

Fig. 1 Calculated heat capacities of (a) MoS_2 and (b) Mo_2S_3 along with the experimental data.

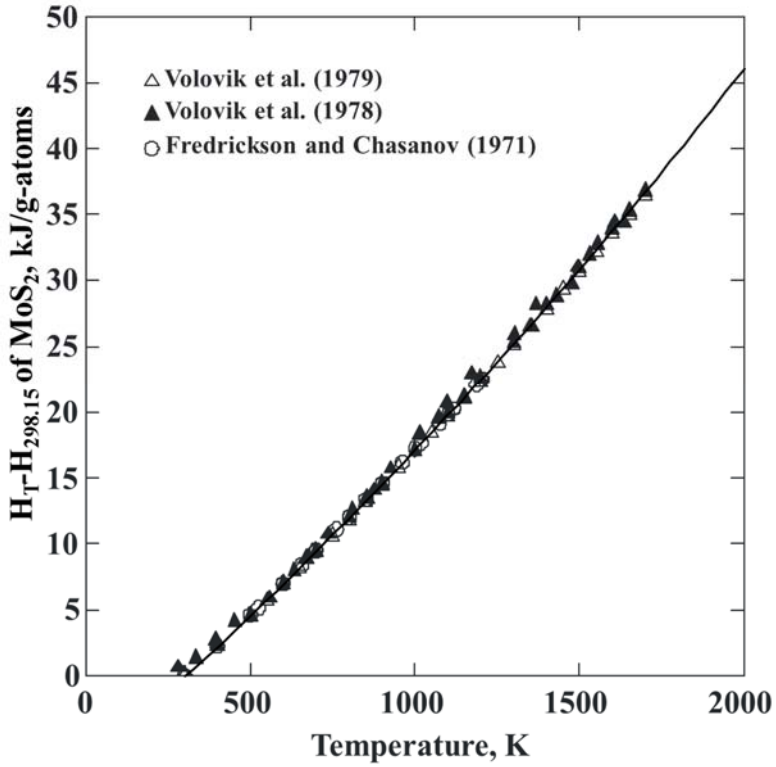

Fig. 2 Calculated heat content of MoS_2 along with the experimental data.

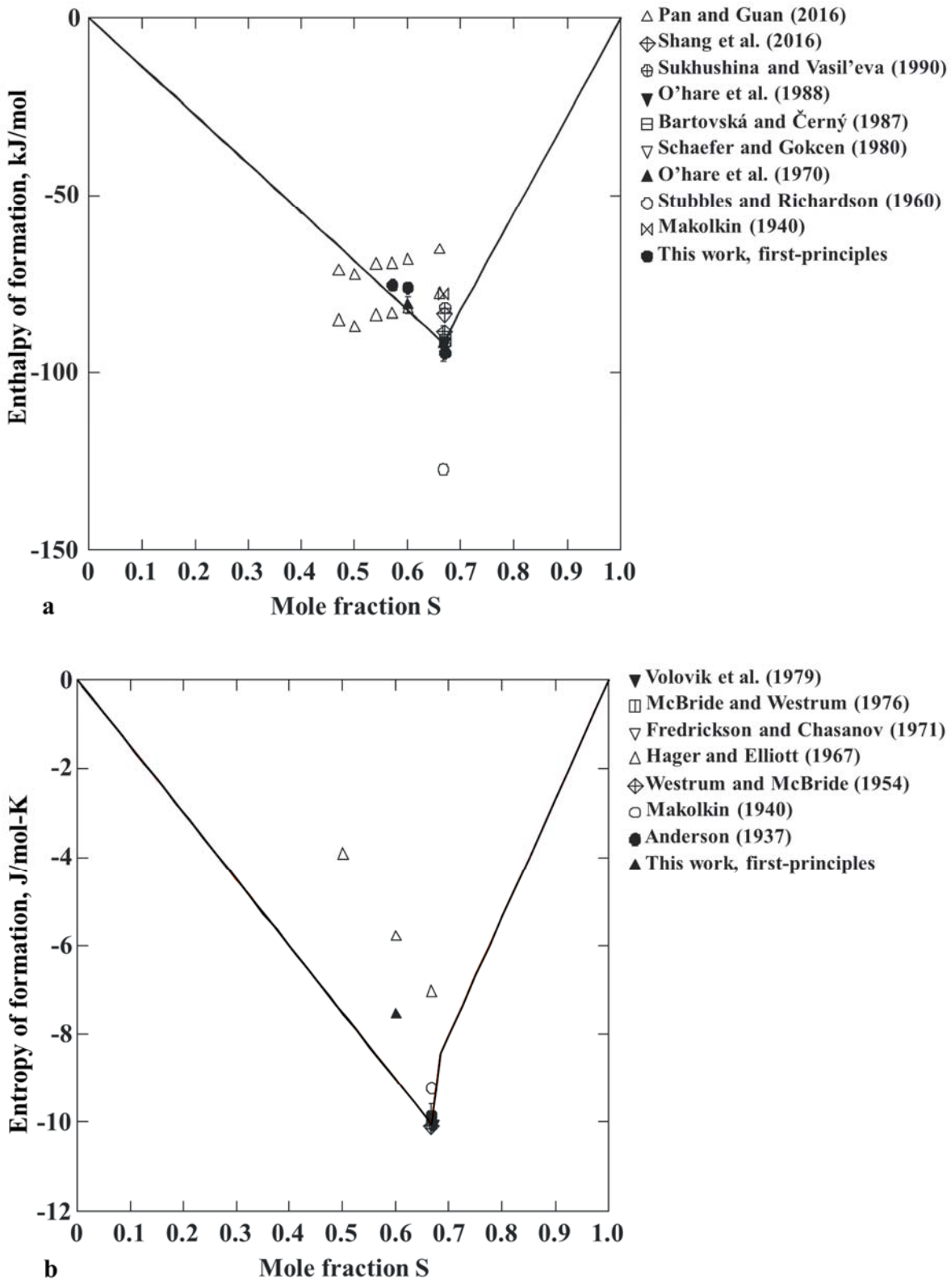

Fig. 3 Calculated (a) enthalpies of formation and (b) entropies of formation of compounds in the Mo-S system at 298.15 K along with the experimental data.

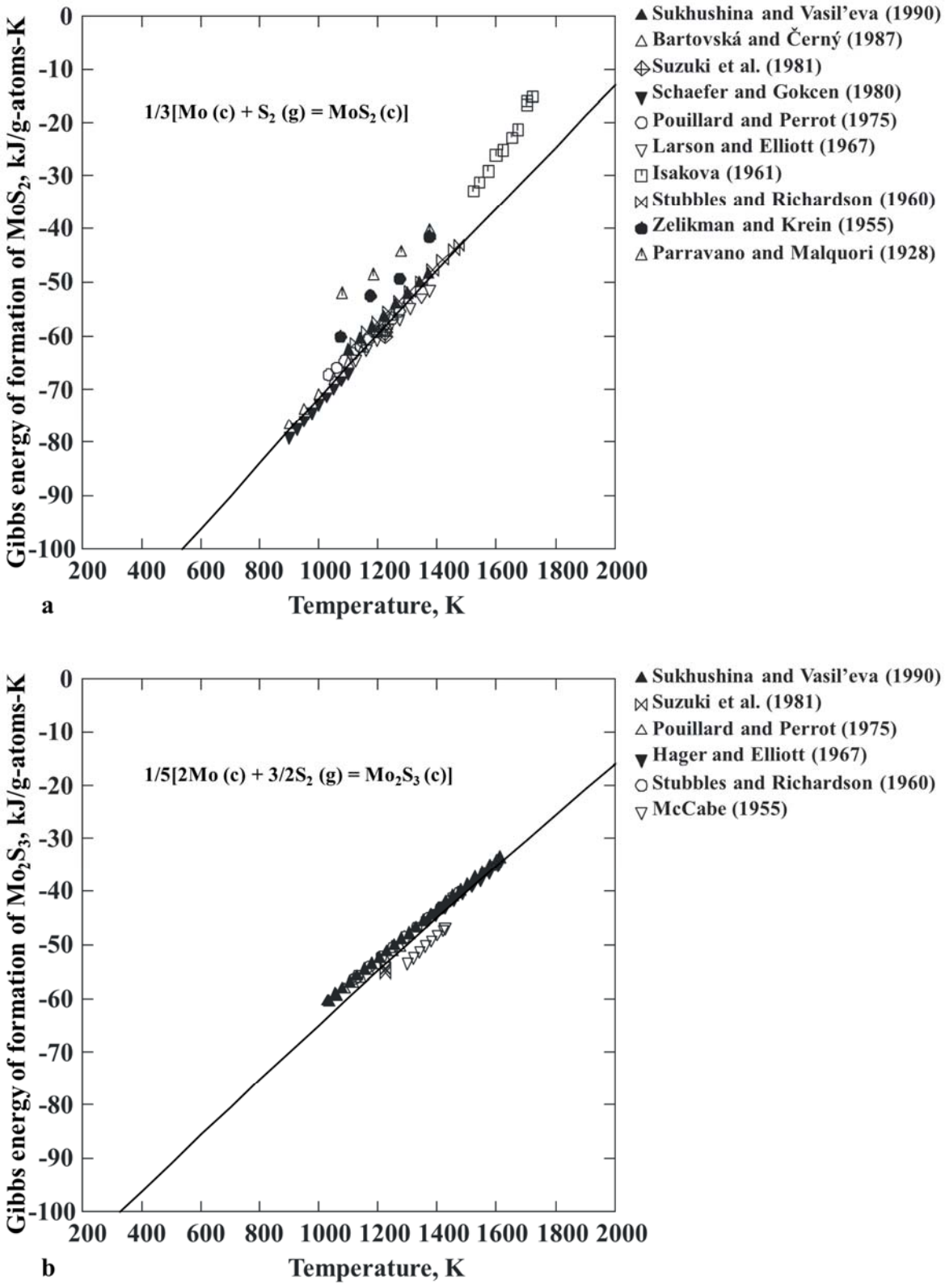

Fig. 4 Calculated Gibbs energies of formation of (a) MoS_2 and (b) Mo_2S_3 along with the experimental data.

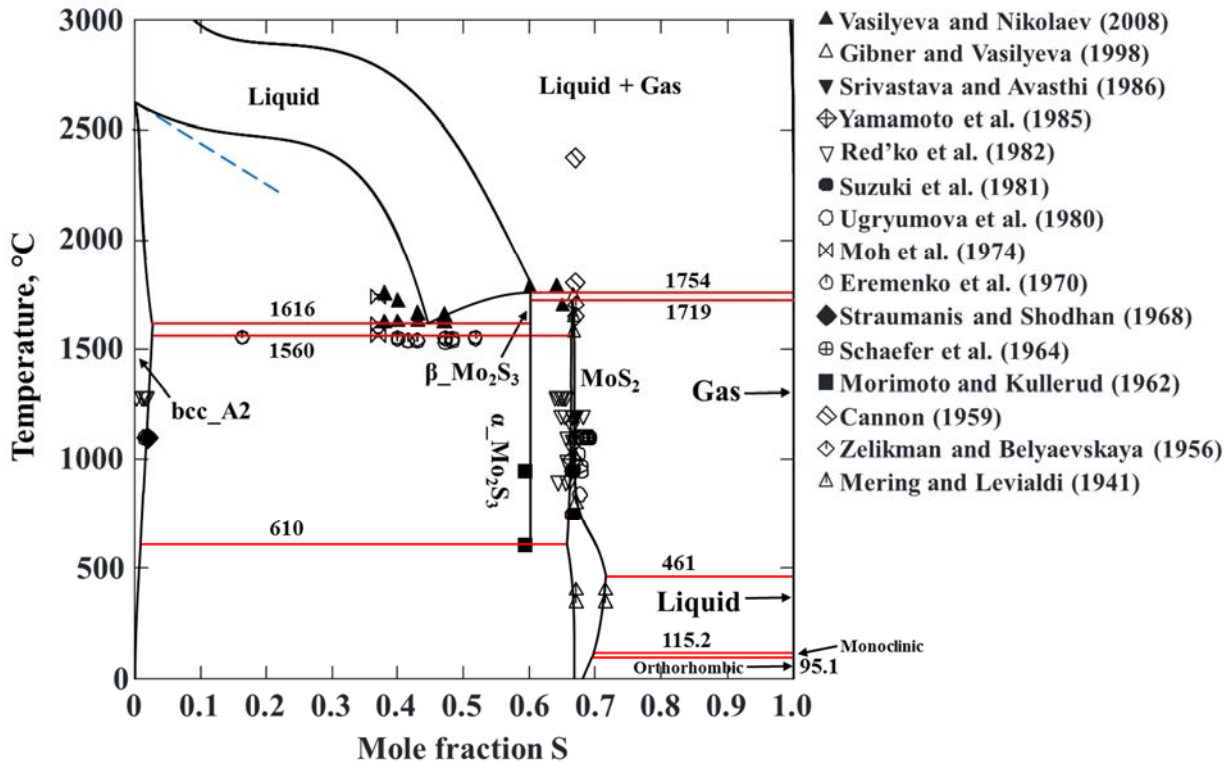

Fig. 5 Calculated Mo-S phase diagram at 1 bar along with the experimental data.

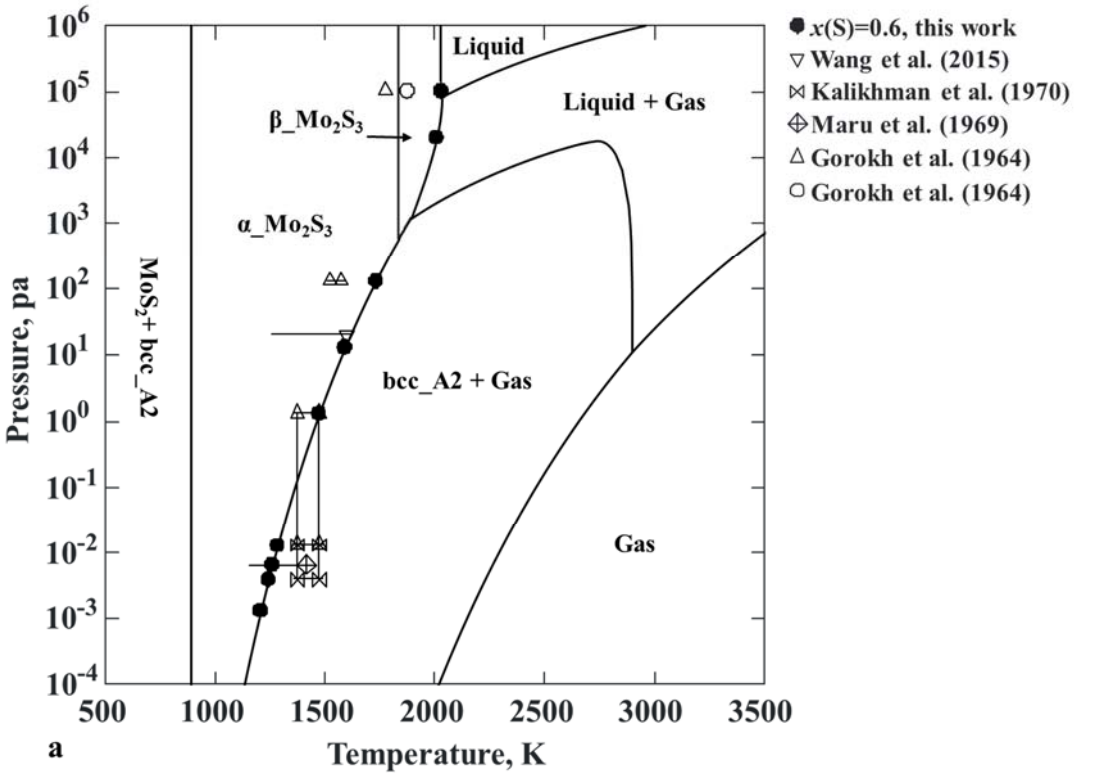
Liquid
Liquid + Gas
β_Mo2S3
α_Mo2S3
MoS2+ bcc_A2
bcc_A2 + Gas
Gas
Pressure, pa
Temperature, K
a
x(S)=0.6, this work
Wang et al. (2015)
Kalikhman et al. (1970)
Maru et al. (1969)
Gorokh et al. (1964)
Gorokh et al. (1964)

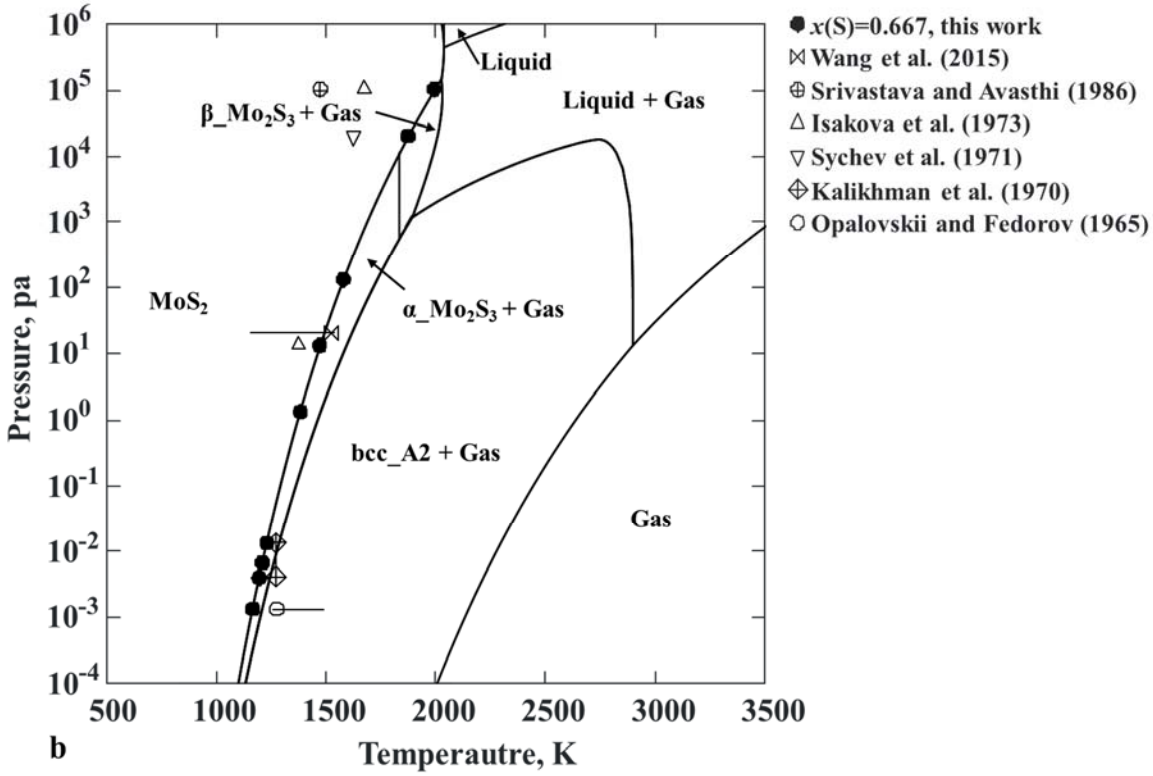
Liquid
Liquid + Gas
β_Mo2S3 + Gas
α_Mo2S3 + Gas
MoS2
bcc_A2 + Gas
Gas
Pressure, pa
Temperautre, K
b
x(S)=0.667, this work
Wang et al. (2015)
Srivastava and Avasthi (1986)
Isakova et al. (1973)
Sychev et al. (1971)
Kalikhman et al. (1970)
Opalovskii and Fedorov (1965)

Fig. 6 Calculated pressure-temperature (*P*-*T*) diagrams along with the experimental data. (a) *x*(S) = 0.6, the experimental data are for Mo_2S_3 = bcc_A2 + gas. (b) *x*(S) = 0.667, the experimental data are for MoS_2 = Mo_2S_3 + gas.

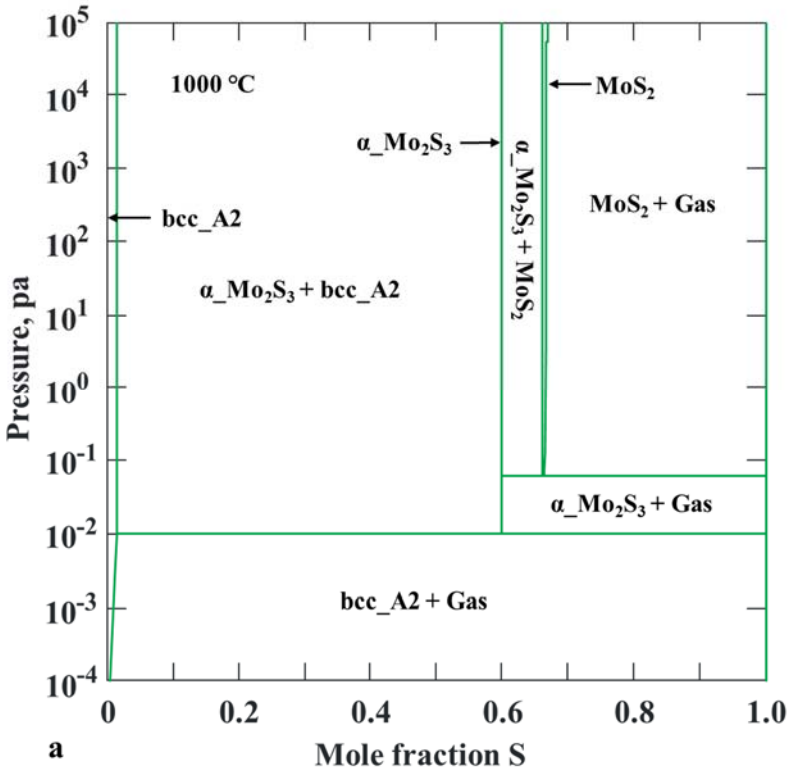
1000 °C
MoS2
α_Mo2S3
α_Mo2S3 + MoS2
MoS2 + Gas
bcc_A2
α_Mo2S3 + bcc_A2
α_Mo2S3 + Gas
bcc_A2 + Gas
Pressure, pa
Mole fraction S
a

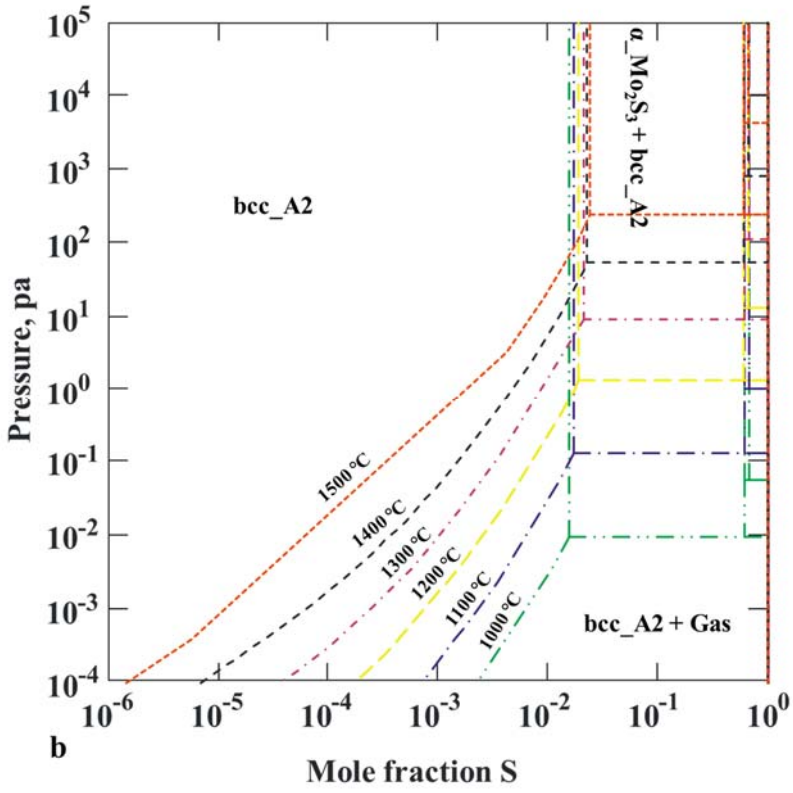
bcc_A2
α_Mo2S3 + bcc_A2
1500 °C
1400 °C
1300 °C
1200 °C
1100 °C
1000 °C
bcc_A2 + Gas
Pressure, pa
Mole fraction S
b

Fig. 7 Calculated pressure-composition (*P*-*x*) diagrams along with the experimental data. (a) 1000 °C, (b) 1000-1500 °C (in logarithm composition scale).

[1] Z.-f. Cao, H. Zhong, G.-y. Liu, Y.-r. Qiu, S. Wang, Molybdenum extraction from molybdenite concentrate in NaCl electrolyte, J. Taiwan Inst. Chem. Eng., 41 (2010) 338-343.
[2] K. Jiang, Y. Wang, X. Zou, L. Zhang, S. Liu, Extraction of Molybdenum from Molybdenite Concentrates with Hydrometallurgical Processing, JOM, 64 (2012) 1285-1289.
[3] G. Li, Z. You, H. Sun, R. Sun, Z. Peng, Y. Zhang, T. Jiang, Separation of rhenium from lead-rich molybdenite concentrate via hydrochloric acid leaching followed by oxidative roasting, Metals (Basel, Switz.), 6 (2016) 282/281-282/212.
[4] J.D. Lessard, D.G. Gribbin, L.N. Shekhter, Recovery of rhenium from molybdenum and copper concentrates during the Looping Sulfide Oxidation process, Int. J. Refract. Met. Hard Mater., 44 (2014) 1-6.
[5] T.W. Scharf, S.V. Prasad, Solid lubricants: a review, J. Mater. Sci., 48 (2013) 511-531.
[6] H. Li, J. Wang, S. Gao, Q. Chen, L. Peng, K. Liu, X. Wei, Superlubricity between MoS2 Monolayers, Adv. Mater. (Weinheim, Ger.), (2017) Ahead of Print.
[7] J.-K. Xiao, W. Zhang, L.-M. Liu, L. Zhang, C. Zhang, Tribological behavior of copper-molybdenum disulfide composites, Wear, 384-385 (2017) 61-71.
[8] B. Radisavljevic, A. Radenovic, J. Brivio, V. Giacometti, A. Kis, Single-layer MoS2 transistors, Nat. Nanotechnol., 6 (2011) 147-150.
[9] A. Verma, W. Jiang, H.H. Abu Safe, W.D. Brown, A.P. Malshe, Tribological behavior of deagglomerated active inorganic nanoparticles for advanced lubrication, Tribol. Trans., 51 (2008) 673-678.
[10] K.F. Mak, K. He, C. Lee, G.H. Lee, J. Hone, T.F. Heinz, J. Shan, Tightly bound trions in monolayer MoS2, Nat. Mater., 12 (2013) 207-211.
[11] A. Molina-Sanchez, K. Hummer, L. Wirtz, Vibrational and optical properties of MoS2: from monolayer to bulk, arXiv.org, e-Print Arch., Condens. Matter, (2016) 1-41.
[12] H. Wang, F. Liu, W. Fu, Z. Fang, W. Zhou, Z. Liu, Two-dimensional heterostructures: fabrication, characterization, and application, Nanoscale, 6 (2014) 12250-12272.
[13] L. Xu, W.-Q. Huang, W. Hu, K. Yang, B.-X. Zhou, A. Pan, G.-F. Huang, Two-Dimensional MoS2-Graphene-Based Multilayer van der Waals Heterostructures: Enhanced Charge Transfer and Optical Absorption, and Electric-Field Tunable Dirac Point and Band Gap, Chem. Mater., 29 (2017) 5504-5512.
[14] L. Dobusch, S. Schuler, V. Perebeinos, T. Mueller, Thermal Light Emission from Monolayer MoS2, Adv. Mater. (Weinheim, Ger.), (2017) Ahead of Print.
[15] E.J. Reed, Piezoelectricity: Now in two dimensions, Nat Nano, 10 (2015) 106-107.
[16] B. Ouyang, S. Xiong, Z. Yang, Y. Jing, Y. Wang, MoS2 heterostructure with tunable phase stability: strain induced interlayer covalent bond formation, Nanoscale, 9 (2017) 8126-8132.
[17] Y. Guo, D. Sun, B. Ouyang, A. Raja, J. Song, T.F. Heinz, L.E. Brus, Probing the Dynamics of the Metallic-to-Semiconducting Structural Phase Transformation in MoS2 Crystals, Nano Letters, 15 (2015) 5081-5088.
[18] B. Ouyang, Z. Mi, J. Song, Bandgap Transition of 2H Transition Metal Dichalcogenides: Predictive Tuning via Inherent Interface Coupling and Strain, The Journal of Physical Chemistry C, 120 (2016) 8927-8935.
[19] Y.-C. Lin, D.O. Dumcenco, Y.-S. Huang, K. Suenaga, Atomic mechanism of the semiconducting-to-metallic phase transition in single-layered MoS2, Nat Nano, 9 (2014) 391-396.

[20] L. Karvonen, A. Saynatjoki, M.J. Huttunen, A. Autere, B. Amirsolaimani, S. Li, R.A. Norwood, N. Peyghambarian, H. Lipsanen, G. Eda, K. Kieu, Z. Sun, Rapid visualization of grain boundaries in monolayer MoS2 by multiphoton microscopy, Nat. Commun., 8 (2017) 15714.
[21] Y. Wang, T. Yao, J.-L. Yao, J. Zhang, H. Gou, Does the real ReN2 have the MoS2 structure?, Phys Chem Chem Phys, 15 (2013) 183-187.
[22] P. Murugan, V. Kumar, Y. Kawazoe, N. Ota, Understanding the Structural Stability of Compound Mo-S Clusters at Sub-Nanometer Level, MATERIALS TRANSACTIONS, 48 (2007) 658-661.
[23] R.C. Che, N. Bai, L.M. Peng, Structure and growth of monoclinic Mo2S3 nanorods, Appl. Phys. Lett., 83 (2003) 3561-3563.
[24] R. Flukiger, R. Baillif, J. Muller, K. Yvon, The constitution diagram of the system copper molybdenum sulfide (CuxMo6S8) in the temperature range 11-2000 K, Journal of the Less-Common Metals, 72 (1980) 193-204.
[25] S.-L. Shang, G. Lindwall, Y. Wang, J.M. Redwing, T. Anderson, Z.-K. Liu, Lateral Versus Vertical Growth of Two-Dimensional Layered Transition-Metal Dichalcogenides: Thermodynamic Insight into MoS2, Nano Lett., 16 (2016) 5742-5750.
[26] F. Liu, Y. Zhou, D. Liu, X. Chen, C. Yang, L. Zhou, Thermodynamic calculations and dynamics simulation on thermal-decomposition reaction of MoS2 and Mo2S3 under vacuum, Vacuum, 139 (2017) 143-152.
[27] L. Wang, P. Guo, J. Pang, L. Luo, P. Zhao, Phase change and kinetics of vacuum decomposition of molybdenite concentrate, Vacuum, 116 (2015) 77-81.
[28] V.V. Sychev, D.Z. Yurchenko, Y.G. Tkachenko, V.A. Obolonchik, S.V. Drozdova, Thermal dissociation of tungsten and molybdenum disulfides; tungsten, molybdenum and niobium diselenides; and boron nitrides in helium, Porosh. Met., 11 (1971) 80-84.
[29] A.V. Gorokh, L.I. Klokotina, K.N. Rispel, Behavior of molybdenite and its dissociation products on heating, Dokl. Akad. Nauk SSSR, 158 (1964) 1183-1185.
[30] S. Cui, I.-H. Jung, Thermodynamic Modeling of the Al-Cr-Mn Ternary System, Metall. Mater. Trans. A, 48 (2017) 1383-1401.
[31] S. Cui, I.-H. Jung, Thermodynamic modeling of the quaternary Al-Cu-Mg-Si system, Calphad, 57 (2017) 1-27.
[32] S. Cui, I.-H. Jung, Thermodynamic assessments of the Cr-Si and Al-Cr-Si systems, J. Alloys Compd., 708 (2017) 887-902.
[33] S. Cui, I.-H. Jung, J. Kim, J. Xin, A coupled experimental and thermodynamic study of the Al-Cr and Al-Cr-Mg systems, J. Alloys Compd., 698 (2017) 1038-1057.
[34] S. Cui, L. Zhang, Y. Du, D. Zhao, H. Xu, W. Zhang, S. Liu, Assessment of atomic mobilities in fcc Cu–Ni–Zn alloys, Calphad, 35 (2011) 231-241.
[35] S. Cui, Y. Du, L. Zhang, Y. Liu, H. Xu, Assessment of atomic mobilities in fcc Al-Zn and Ni-Zn alloys, Calphad, 34 (2010) 446-451.
[36] G. Kresse, J. Furthmiiller, Efficiency of ab-initio total energy calculations for metals and semiconductors using a plane-wave basis set, Comp. Mater. Sci., 6 (1996) 15-50.
[37] G. Kresse, J. Furthmüller, Efficient iterative schemes for ab initio total-energy calculations using a plane-wave basis set, Phys. Rev. B, 54 (1996) 11169-11186.
[38] G. Kresse, D. Joubert, From ultrasoft pseudopotentials to the projector augmented-wave method, Phys. Rev. B, 59 (1999) 1758-1775.
[39] P.E. Blöchl, Projector augmented-wave method, Phys. Rev. B, 50 (1994) 17953-17979.
[40] J.P. Perdew, K. Burke, M. Ernzerhof, Generalized Gradient Approximation Made Simple, Phys. Rev. Lett., 77 (1996) 3865.
[41] H.J. Monkhorst, J.D. Pack, Special points for Brillouin-zone integrations, Phys. Rev. B, 13 (1976) 5188-5192.

[42] P.E. Blöchl, O. Jepsen, O.K. Andersen, Improved tetrahedron method for Brillouin-zone integrations, Phys. Rev. B, 49 (1994) 16223-16233
[43] A. Togo, L. Chaput, I. Tanaka, G. Hug, First-principles phonon calculations of thermal expansion in Ti3SiC2, Ti3AlC2, and Ti3GeC2, Physical Review B, 81 (2010) 174301.
[44] A. Togo, F. Oba, I. Tanaka, First-principles calculations of the ferroelastic transition between rutile-type and CaC2-type SiO2 at high pressures, Physical Review B, 78 (2008) 134106.
[45] C.T. Anderson, The heat capacities of molybdenite and pyrite at low temperatures, J. Am. Chem. Soc., 59 (1937) 486-487.
[46] D.F. Smith, D. Brown, A.S. Dworkin, D.J. Sasmor, E.R. Van Artsdalen, Low-temperature heat capacity and entropy of molybdenum trioxide and molybdenum disulfide, J. Am. Chem. Soc., 78 (1956) 1533-1536.
[47] H.L. Kiwia, E.F. Westrum, Low-temperature heat capacities of molybdenum diselenide and ditelluride, The Journal of Chemical Thermodynamics, 7 (1975) 683-691.
[48] J.J. McBride, E.F. Westrum, Low-temperature heat capacity of anisotropic crystals lamellar molybdenum disulfide, The Journal of Chemical Thermodynamics, 8 (1976) 37-44.
[49] D.R. Fredrickson, M.G. Chasanov, Enthalpy of molybdenum disulfide to 1200.deg.K by drop calorimetry, J. Chem. Thermodyn., 3 (1971) 693-696.
[50] L.S. Volovik, L.N. Bazhenova, A.S. Bolgar, L.A. Klochkov, S.V. Drozdova, V.F. Primachenko, I.I. Timofeeva, Thermodynamic properties of transition metal sulfides, Izv. Akad. Nauk SSSR, Neorg. Mater., 15 (1979) 638-642.
[51] L.S. Volovik, V.V. Fesenko, A.S. Bolgar, S.V. Drozdova, L.A. Klochkov, V.F. Primachenko, Enthalpy and heat capacity of molybdenum disulfide, Poroshk. Metall. (Kiev), (1978) 54-59.
[52] J. Yuan, Z. Lv, Q. Lu, Y. Cheng, X. Chen, L. Cai, First-principles study of the phonon vibrational spectra and thermal properties of hexagonal MoS2, Solid State Sci., 40 (2015) 1-6.
[53] K. Ali, Y. Haluk, K. Alper, Ç. Tahir, S. Cem, Thermal transport properties of MoS 2 and MoSe 2 monolayers, Nanotechnology, 27 (2016) 055703.
[54] E.F. Westrum, J.J. McBride, Temperature dependence of heat capacity of Molybdenite, Bulletin of the American Physical Society, 29 (1954) 22.
[55] I.A. Makolkin, Free energy and the heat of formation of molybdenum disulfide from measurements of the electromotive forces, Zh. Fiz. Khim., 14 (1940) 110-112.
[56] J.P. Hager, J.F. Elliott, The free energies of formation of CrS, Mo2S3, and WS2., Transcations of the AIME, 239 (1967) 513-520.
[57] P.A.G. O'Hare, E. Benn, F.Y. Cheng, G. Kuzmycz, Fluorine bomb calorimetric study of molybdenum disulfide. Standard enthalpies of formation of the di- and sesquisulfides of molybdenum, J. Chem. Thermodyn., 2 (1970) 797-804.
[58] P.A.G. O'Hare, B.M. Lewis, B.A. Parkinson, Standard molar enthalpy of formation by fluorine-combustion calorimetry of tungsten diselenide (WSe2). Thermodynamics of the high-temperature vaporization of tungsten diselenide. Revised value of the standard molar enthalpy of formation of molybdenite (MoS2), J. Chem. Thermodyn., 20 (1988) 681-691.
[59] I.S. Sukhushina, I.A. Vasil'eva, Thermodynamic properties of molybdenite, Geokhimiya, (1990) 1063-1068.
[60] L. Bartovska, C. Cerny, Chemical equilibria in heterogeneous systems. Part X. The influence of the structure of molybdenum disulfide on its reactivity, Collect. Czech. Chem. Commun., 52 (1987) 678-685.
[61] S.C. Schaefer, Electrochemical determination of Gibbs energies of formation of molybdenum disulfide and tungsten disulfide, in, Bur. Mines, 1980, pp. 17 pp.
[62] S.C. Schaefer, N.A. Gokcen, Electrochemical determination of thermodynamic properties of molybdenite (MoS2), High Temp. Sci., 12 (1980) 267-276.

[63] J.R. Stubbles, F.D. Richardson, Equilibriums in the system molybdenum + sulfur + hydrogen, Trans. Faraday Soc., 56 (1960) 1460-1466.
[64] Y. Pan, W. Guan, Effect of sulfur concentration on structural, elastic and electronic properties of molybdenum sulfides from first-principles, Int. J. Hydrogen Energy, 41 (2016) 11033-11041.
[65] G. Pouillard, P. Perrot, Free enthalpy of formation and region of stability of molybdenum(III) and molybdenum(IV) sulfide, Comptes Rendus des Seances de l'Academie des Sciences, Serie C: Sciences Chimiques, 281 (1975) 143-146.
[66] H.R. Larson, J.F. Elliott, Standard free energy of formation of certain sulfides of some transition elements and zinc, Transactions of the American Institute of Mining, Metallurgical and Petroleum Engineers, 239 (1967) 1713-1720.
[67] Y. Suzuki, T. Uchida, M. Wakihara, M. Taniguchi, Phase relationship in molybdenum-sulfur system at high temperatures, Materials Research Bulletin, 16 (1981) 1085-1090.
[68] A.N. Zelikman, O.E. Krein, Thermal dissociation of molybdenum disulfide, Zh. Fiz. Khim., 29 (1955) 2081-2085.
[69] N. Parravano, G. Malquori, Researches on molybdenum sulfides. II. Equilibrium of reduction of molybdenum bisulfide by means of hydrogen, Alli accad. Lincei [6], 7 (1928) 109-112.
[70] N. Parravano, G. Malquori, Researches on molybdenum sulfides. I. The vapor pressures of the sulfur of molybdenum trisulfide, Alli accad. Lincei [6], 7 (1928) 19-22.
[71] R.A. Isakova, Vapor and dissociation pressures of molybdenite, Izvest. Akad. Nauk Kazakh. S.S.R., Ser. Met., Obogashchen. i Ogneuporov, No. 3 (1961) 3-10.
[72] C.L. McCabe, Sulfur pressure measurements of molybdenum sesquisulfide in equilibrium with molybdenum, J. Met., 7 (1955) 61-63.
[73] S. Takeno, G.H. Moh, Liquidus reactions of the Mo-S system, Neues Jahrb. Mineral., 131 (1977) 43-48.
[74] G.H. Moh, High-temperature metal sulfide chemistry, in: Topics in Current Chemistry: Aspects of Molybdenum and Related Chemistry, Springer Berlin Heidelberg, Berlin, Heidelberg, 1978, pp. 107-151.
[75] L. Brewer, R.H. Lamoreaux, Mo-S, Bull. Alloy Phase Diagrams, 93 (1980) 93-95.
[76] W.B. Johnson, W.S. Hong, D.W. Readey, A molybdenum-sulfur binary phase diagram, Scripta Metallurgica, 17 (1983) 919-922.
[77] V.V. Starkov, D.V. Drobot, E.A. Pisarev, A.N. Zelikman, The molybdenum-sulfur system, Izvestiya Vysshikh Uchebnykh Zavedenii, Tsvetnaya Metallurgiya, (1987) 51-57.
[78] A.V. Gorokh, L.N. Rusakov, A.A. Savinskaya, Synthesis and characteristics of molybdenum sesquisulfide, Dokl. Akad. Nauk SSSR, 156 (1964) 541-542.
[79] N. Morimoto, G. Kullerud, Ore minerals. The Mo-S system, Year Book - Carnegie Institution of Washington, 1961 (1962) 143-144.
[80] S.C. Schaefer, A.H. Larson, A.W. Schlechten, Sulfur pressure variation of molybdenum disulfide at 1100°, Transactions of the American Institute of Mining, Metallurgical and Petroleum Engineers, 230 (1964) 594-595.
[81] G. Krabbes, H. Oppermann, J. Henke, Chemischer Transport und thermische Stabilität von Sulfidphasen des Molybdäns, Zeitschrift für anorganische und allgemeine Chemie, 470 (1980) 7-17.
[82] I.G. Vasilyeva, R.E. Nikolaev, High-temperature solid-vapor and liquid-vapor transitions in binary and ternary chalcogenides La2S3, MoS2, Mo2S3 and LiInSe2, J. Alloys Compd., 452 (2008) 89-93.
[83] Y.I. Gibner, I.G. Vasilyeva, Rapid Heating in High-Temperature Thermomicroscopic Analysis, Journal of Thermal Analysis and Calorimetry, 53 (1998) 151-160.
[84] G.H. Moh, G. Udubasa, R. Hueller, High temperature phase equilibriums in the molybdenum-sulfur system, Metall (Isernhagen, Germany), 28 (1974) 804.
[85] G.H. Moh, High-temperature metal sulfide chemistry, (1978).

[86] Y. Han, Molybdenite polytypes and mechanism of polytype formation, Diqiu Kexue, 13 (1988) 385-394.
[87] L.A. Arutyunyan, E.K. Khurshudyan, Synthesis of molybdenum disulfide from thiomolybdate solutions at elevated temperature, Geokhimiya, (1966) 650-658.
[88] A.N. Zelikman, Y.D. Christyakov, G.V. Indenbaum, O.E. Krein, Crystal structure of molybdenum disulfide prepared by different methods, Kristallografiya, 6 (1961) 389-394.
[89] A.N. Zelikman, G.V. Indenbaum, M.V. Teslitskaya, V.P. Shalankova, Structural transformations of synthetic molybdenum disulfide, Kristallografiya, 14 (1969) 795-799.
[90] M.O. Rikel, Z.M. Alekseeva, Phase relations in the lead-molybdenum-sulfur system in the 900-1150° and 13.3-266 gPa ranges, Izv. Akad. Nauk SSSR, Neorg. Mater., 17 (1981) 2089-2094.
[91] A.H. Clark, Compositional differences between hexagonal and rhombohedral molybdenite, Neues Jahrbuch fuer Mineralogie, Monatshefte, (1970) 33-38.
[92] R.J.J. Newberry, Polytypism in molybdenite (I): a non-equilibrium impurity-induced phenomenon, Am. Mineral., 64 (1979) 758-767.
[93] R.J.J. Newberry, Polytypism in molybdenite (II): relationships between polytypism, ore deposition/alteration stages and rhenium contents, Am. Mineral., 64 (1979) 768-775.
[94] H. Rau, Estimation of the homogeneity range of molybdenum disulfide, J. Phys. Chem. Solids, 41 (1980) 765-767.
[95] S. Yamamoto, M. Wakihara, M. Taniguchi, Phase relations in the lead-molybdenum-sulfur ternary system at 1000°C and the superconductivity of lead molybdenum sulfide (PbxMo6S8-y), Materials Research Bulletin, 20 (1985) 1493-1500.
[96] L.E. Ugryumova, V.A. Snurnikova, R.A. Isakova, V.P. Bystrov, A.V. Vanyukov, I.A. Sapukov, Molybdenum disulfide dissociation pressure, Zh. Prikl. Khim. (Leningrad), 51 (1978) 2684-2687.
[97] A.I. Red'ko, V.A. Spitsyn, L.E. Ugryumova, I.A. Sapukov, R.A. Isakova, Phase equilibrium in the molybdenum-sulfur system, Izv. Akad. Nauk Kaz. SSR, Ser. Khim., (1982) 10-15.
[98] J. Mering, A. Levialdi, Molybdenum sulfides, Compt. rend., 213 (1941) 798-800.
[99] E.Y. Rode, B.A. Lebedev, Physicochemical study of molybdenum trisulfide and products of its thermal decomposition, Zh. Neorg. Khim., 6 (1961) 1189-1203.
[100] P. Cannon, Melting point and sublimation of molybdenum disulfide, Nature (London, U. K.), 183 (1959) 1612-1613.
[101] A.N. Zelikman, L.V. Belyaevskaya, The melting point of molybdenite, Zh. Neorg. Khim., 1 (1956) 2239-2244.
[102] http://www.thermocalc.com/products-services/databases/thermodynamic/.
[103] V.N. Eremenko, V.E. Listovnichii, A.A. Opalovskii, V.E. Fedorov, Physicochemical study of the molybdenum-sulfur system, Khal'kogenidy, No. 2 (1970) 92-97.
[104] F. Mawrow, M. Nokolow, New sulfides of molybdenum, Z. Anorg. Allg. Chem., 95 (1916) 188-193.
[105] D.E. Wilcox, L.A. Bromley, Computer estimation of heat and free energy of formation for simple inorganic compounds, Ind. Eng. Chem., 55 (1963) 32-39.
[106] P. Ratnasamy, L. Rodrique, A.J. Leonard, Structural and textural studies in molybdenum sulfide systems, The Journal of Physical Chemistry, 77 (1973) 2242-2245.
[107] M.I. Ermolaev, S.M. Basitova, N.A. Shatkovskaya, DTA and differential thermogravimetric analysis of rhenium and molybdenum sulfides, Dokl. Akad. Nauk Tadzh. SSR, 18 (1975) 27-29.
[108] J.C. Wildervanck, F. Jellinek, Preparation and crystallinity of molybdenum and tungsten sulfides, Z. Anorg. Allg. Chem., 328 (1964) 309-318.
[109] M. Stemprok, Bismuth-molybdenum-sulfur system, Year Book - Carnegie Institution of Washington, 65 (1967) 336-337.
[110] R. Chevrel, M. Sergent, J. Prigent, New molybdenum sulfide, Mo3S4. Preparation, properties, and crystal structure, Materials Research Bulletin, 9 (1974) 1487-1498.

[111] R. Flukiger, H. Devantay, J. Jorda, J. Muller, Metallurgical and physical properties of ternary Molybdenum Sulfides (M<inf>x</inf>Mo<inf>3</inf>S<inf>4</inf>) as synthetized in the bulk state, IEEE Transactions on Magnetics, 13 (1977) 818-820.
[112] M.E. Straumanis, R.P. Shodhan, Lattice constants, thermal expansion coefficients, and densities of molybdenum and the solubility of sulfur, selenium, and tellurium in it at 1100.deg, Z. Metallk., 59 (1968) 492-495.
[113] A.T. Dinsdale, SGTE data for pure elements, CALPHAD: Computer Coupling of Phase Diagrams and Thermochemistry, 15 (1991) 317-425.
[114] H. Okamoto, T.B. Massalski, Thermodynamically Improbable Phase Diagrams, Journal of Phase Equilibria, 12 (1991) 148-168.
[115] R.A. Isakova, L.E. Ugryumova, K.S. Amosova, N.A. Potanina, Behavior of molybdenum disulfide during heating in vacuo, Izv. Akad. Nauk Kaz. SSR, Ser. Khim., 23 (1973) 6-10.
[116] A.A. Opalovskii, V.E. Fedorov, Thermal dissociation of molybdenum disulfide in vacuum, Dokl. Akad. Nauk SSSR, 163 (1965) 900-901.
[117] V.L. Kalikhman, S.V. Radzikovskaya, V.F. Bukhanevich, E.P. Gladchenko, In vacuo behavior of tungsten, molybdenum, niobium, and tantalum sulfides, Porosh. Met., 10 (1970) 55-60.
[118] Y. Maru, ocirc, ichi, H. Yoshida, Kond, ocirc, Yoshio, On the Thermal Decomposition Rate of Molybdenum Sesquisulphide (Mo₂S₃) in Vacuum, Transactions of the Japan Institute of Metals, 10 (1969) 8-11.
[119] S.K. Srivastava, B.N. Avasthi, High pressure synthesis and characterization of molybdenum disulfide, Journal of the Less-Common Metals, 124 (1986) 85-92.
[120] O. Redlich, A.T. Kister, Thermodynamics of nonelectrolytic solutions. Algebraic representation of thermodynamic properties and the classification of solutions, Industrial and Engineering Chemistry, 40 (1948) 84,85-88.
[121] M. Hillert, M. Jarl, A model for alloying effects in ferromagnetic metals, CALPHAD: Computer Coupling of Phase Diagrams and Thermochemistry, 2 (1978) 227-238.
[122] B. Sundman, J. Aagren, A regular solution model for phases with several components and sublattices, suitable for computer applications, Journal of Physics and Chemistry of Solids, 42 (1981) 297-301.
[123] http://www.thermocalc.com.
[124] M.C.L. Patterson, L.J.R. Cohen, J.A. Charles, Studies in the system molybdenum-sulfur, Trans. - Inst. Min. Metall., Sect. C, 96 (1987) C98-C102.